



NEDO-24781-1
80 NED005
CLASS I
JANUARY 1980
CREARE-TN-307

MARK II CONTAINMENT PROGRAM
TASK A.II, PHASE I

COMPARISON OF SINGLE AND MULTIVENT CHUGGING AT TWO SCALES

Bharatan R. Patel
Francis X. Dolan
James A. Block

This document was prepared for the Mark II Utility Owners' Group by Creare Incorporated under contract with the General Electric Company.

Creare INC.
SCIENCE AND TECHNOLOGY

HANOVER, NEW HAMPSHIRE

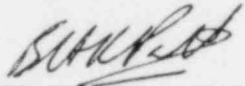
8 007220 334

NEDO-24781-1
80NED005
Class I
January 1980
Creare TN-307

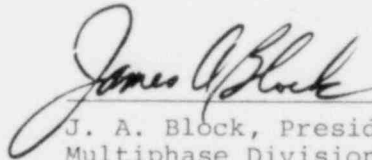
Mark II Containment Program
Task A.11, Phase 1

COMPARISON OF SINGLE AND MULTIVENT
CHUGGING AT TWO SCALES

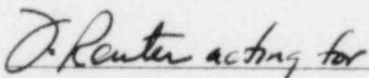
Bharata. R. Patel - Creare Inc.
Francis X. Dolan - Creare Inc.
James A. Block - Creare Inc.



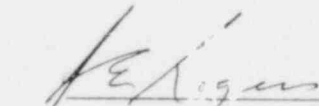
B. R. Patel, Project Director
Creare Incorporated



J. A. Block, President,
Multiphase Division
Creare Incorporated



P. W. Ianni, Manager
Containment Design
General Electric Company



A. E. Rogers, Manager
Containment Technology
General Electric Company

This document was prepared for the Mark II Utility Owner's Group by Creare Inc.
under contract with the General Electric Company.

DISCLAIMER OF RESPONSIBILITY

The only undertakings of the General Electric Company respecting information in this document are contained in the contracts for Mark II Containment Consulting Services between the General Electric Company and each of the members of the U.S. Mark II Owners Group, effective variously June 9, 1975, June 13, 1975, and July 29, 1975, and nothing contained in this document shall be construed as changing the contracts. The use of this information by anyone other than the members of the U.S. Mark II Owners Group either themselves or through their technical consultants, or for any purpose other than that for which it is intended under the contracts, is not authorized; and with respect to any unauthorized use, the General Electric Company makes no representation or warranty, express or implied, and assumes no liability of any kind as to the completeness, accuracy, usefulness or non-infringing nature of the information contained in this document.

ABSTRACT

This is a data report for the Scaled Multivent Test Program Phase 1 single and multivent chugging tests performed at Creare for the Mark II Utility Owners' Group under the direction of the General Electric Company. This report contains an overview of the Multivent Program along with a description of the Phase 1 test facility, test geometries, instrumentation, data acquisition and reduction system and test procedures. The 1/10 and 1/6 scale single vent chugging results are presented; these provided the baseline data for comparisons against multivent data at these scales. Results are also presented from additional single vent tests which were performed to evaluate the effect of drywell volume, pool size and vent location in the pool. The multivent geometries tested in Phase 1 were the 1/10 scale 3 and 7 vent geometries and the 1/6 scale 3 vent geometry, and results from these tests are presented and discussed. The testing was performed over a wide range of thermodynamic parameters, including wetwell airspace pressure, vent steam mass flux, pool temperature and steam air-content. The overall result of these tests is that the wall loads decrease as the number of vents is increased.

EXECUTIVE SUMMARY

This interim report presents data obtained in Phase I of the Scaled Multivent Test Program, a program being performed by Creare Incorporated for the Mark II Utility Owners' Group under the direction of the General Electric Company.

The objectives of the Scaled Multivent Test Program are to: (1) demonstrate that single cell loads are bounding by establishing that multivent loads are less than single vent loads, (2) determine the trend in loads with number of vents and demonstrate validity by experiments at several scales, and (3) obtain data which may be used to confirm analytical application methods. The program contains single vent tests at four scales (with CONMAP and 4T providing fifth and sixth scales) and multivent tests at two scales as summarized in Table S-1. Data from a portion of the 1/10 and 1/6 scale tests are presented in this report.

The five test vessels used ranged in size from 10 in. to 44 in. diameter. All geometries had the drywell-over-wetwell configuration of Mark II plants with straight vents. Critical dimensions such as submergence, clearance, vent diameter, vent spacing and wetwell diameter were linearly scaled; vent lengths and the pool-to-vent area ratio were kept constant between geometries. Special tests in this program, together with previous programs, provide data on the effects of varying these dimensions. In this program, chugging data were obtained over a wide range of conditions (steam flux, air content, pressure, pool temperature) to contribute to basic understanding of the physics of the phenomena and hence the effect of scale and the extension of the data to full scale.

<u>TABLE S-1</u> <u>SCALED MULTIVENT TEST PROGRAM</u>	
Single Vent Test Geometries	1/10*, 1/6*, 1/4, 5/12 scales
Multivent Test Geometries	1/10 scale 3*, 7*, 19 vents 1/6 scale 3*, 7 vents
Additional Test Geometries	Effect of drywell volume* Effect of pool size* Effect of vent location in the pool* Effect of vent length
Total Number of Test Geometries = 19 Total Number of Tests = 749	
*Test performed in Phase I.	

Extensive instrumentation, together with a 28 channel analog tape recorder and a 64 channel minicomputer-based data acquisition and reduction system, provided data on pool interior and boundary pressures; pool temperature distribution; vent pressures; water position and velocity in the vents; vent, vessel and basemat accelerations; and the various steady-state test conditions such as steam and air flow rates, system pressure and pool temperature and depth. Data reduction was accomplished by manually-guided computer manipulations.

The main result from Phase 1 is that the mean pool boundary pressures decrease with increasing number of vents. This is shown to result principally from out-of-phase chugging and the effectively larger pool which therefore results.

Single vent tests at 1/10 and 1/6 scale confirmed, clarified and extended previously observed trends. Figures S-1, S-2, and S-3 qualitatively summarize key single-vent trends; data presented in the body of this report confirm these clearly-established mean value trends despite the randomness of chugging. The single vent data demonstrate that:

- Mean peak overpressure (POP) and underpressure (PUP) increase with steam mass flux (Figure S-1).
- Mean chug frequency (the inverse of the mean period between chugs) is directly proportional to the steam mass flux.
- Mean POP increases with pool temperature, peaks and then decreases as saturation conditions are approached (Figure S-2). Mean PUP decreases continuously as pool temperature increases, and chug period was relatively unaffected by pool temperature over the range tested.

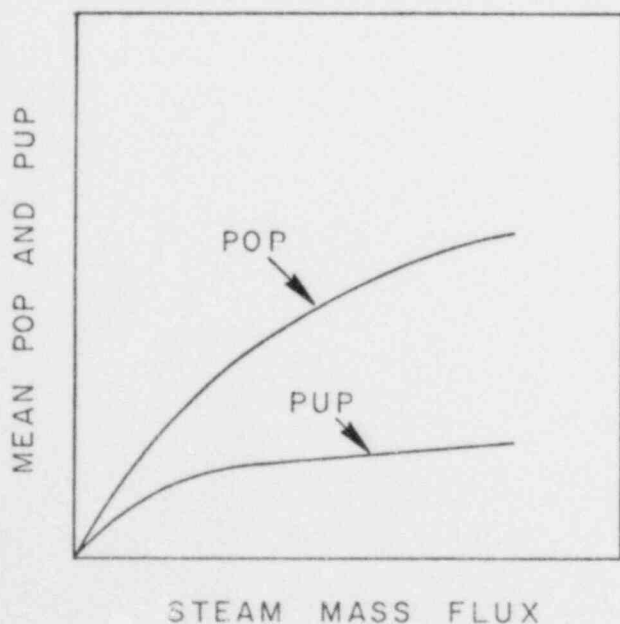


Figure S-1. VARIATION OF MEAN POP AND PUP WITH STEAM MASS FLUX

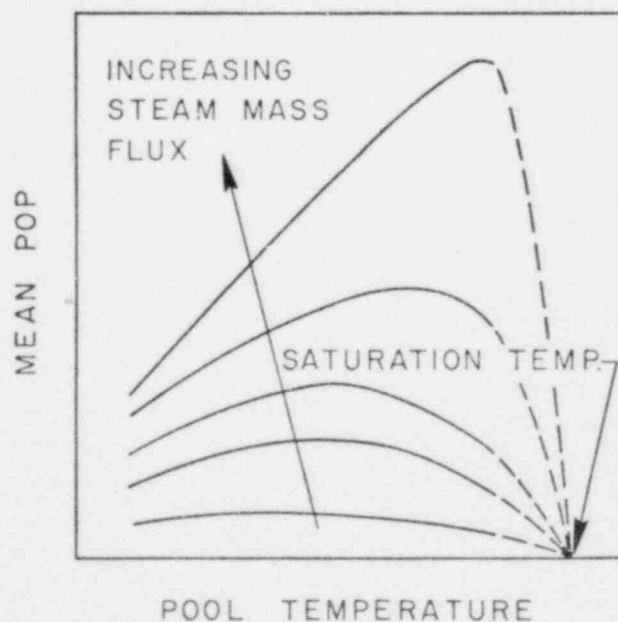


Figure S-2. VARIATION OF MEAN POP WITH POOL TEMPERATURE

- Mean POP and PUP decrease rapidly with air content in the steam (Figure S-3) while chug period is not significantly affected.
- Drywell volume has no significant effect on mean POP, PUP or chug period.
- Mean POP is inversely proportional to pool area. The decrease in mean POP with pool area results from increases both in pool size and distance from the vent to the pressure transducer as verified by special offset-vent tests. These results contribute significantly to understanding of multivent effects and may be utilized to verify pool wave propagation models.

With multiple vents, the effects of the independent thermal and fluid parameters on POP, PUP, and chug period were similar to those observed in the single vent tests. However, multivent mean POP and PUP values were lower than in the corresponding single vent tests. The multivent multiplier decreased with increasing number of vents (Figure S-4). Vent phasing data revealed three vents would typically chug out-of-phase by about 20 ms. Since the physical pool-to-vent area ratio was the same for the multivent tests as the single vent tests, the out-of-phase chugging resulted in each vent chugging in an effectively larger pool thus producing the lower load observed.

Phase 1 has significantly advanced the objectives of this program. Phase 2 will provide key single vent data at two larger scales (1/4 and 5/12) and multivent data with larger number of vents (7 at 1/6 scale and 19 at 1/10 scale).

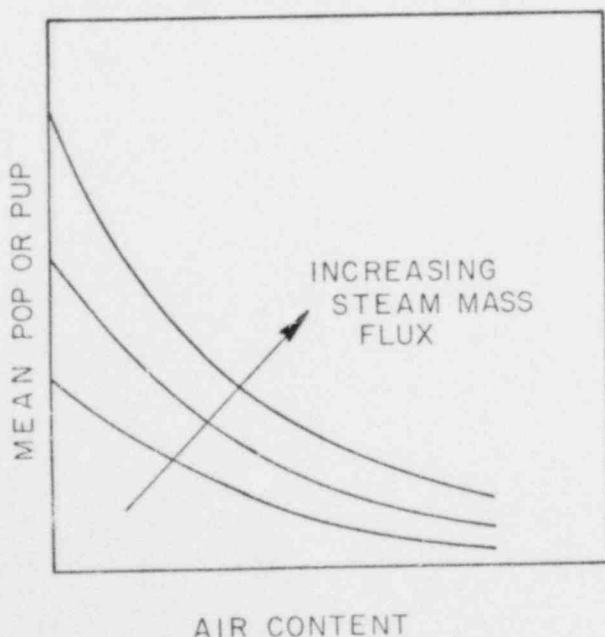


Figure S-3. VARIATION OF MEAN POP AND PUP WITH STEAM AIR-CONTENT

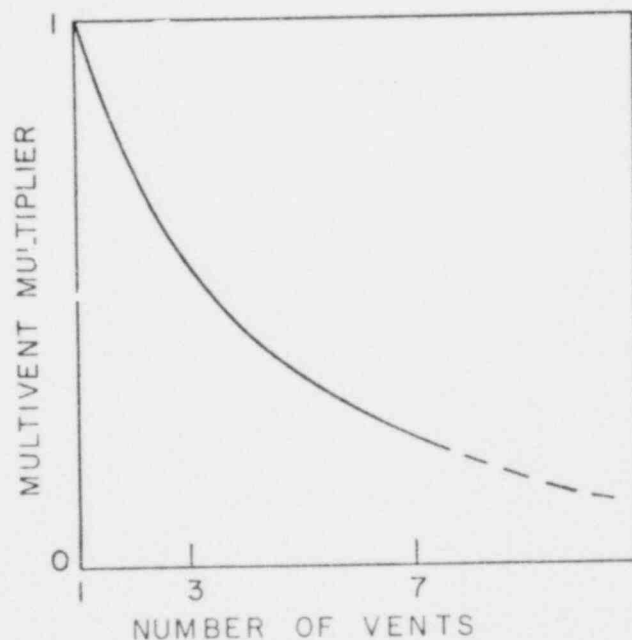


Figure S-4. VARIATION OF MULTIVENT MULTIPLIER WITH NUMBER OF VENTS

TABLE OF CONTENTS

	<u>Page</u>
ABSTRACT	i
EXECUTIVE SUMMARY	ii
TABLE OF CONTENTS	v
1 INTRODUCTION	1-1
1.1 Background	1-1
1.2 Scaled Multivent Test Program Overview	1-3
2 TEST FACILITY AND INSTRUMENTATION	2-1
2.1 Test Facility and Geometries	2-1
2.2 Test Procedures	2-10
2.3 Instrumentation	2-10
2.3.1 Principal Data	2-11
2.3.2 System Data	2-14
2.3.3 Instrument Calibration and Measurement and Accuracy	2-15
3 DATA ACQUISITION AND REDUCTION PROCEDURES	3-1
3.1 Data Acquisition System and Procedures	3-1
3.2 Data Reduction	3-1
3.2.1 Wall Pressure Data Reduction	3-5
3.2.2 Vent Phasing Data Reduction	3-7
4 TEST MATRIX	4-1
5 TEST RESULTS AND DISCUSSION—SINGLE VENT DATA AT 1/10 AND 1/6 SCALE	5-1
5.1 Effect of Steam Mass Flux	5-7
5.2 Effect of Pool Temperature	5-17
5.3 Effect of Air	5-37
5.4 Effect of Drywell Volume	5-53
5.5 Effect of Pool Size	5-57
5.6 Effect of Vent Offset	5-66
6 TEST RESULTS AND DISCUSSION—MULTIVENT DATA AT 1/10 AND 1/6 SCALE	6-1
6.1 Multivent Pool Wall Pressures	6-1
6.2 Vent Phasing	6-34
6.3 Effect of Drywell Volume	6-46
7 CONCLUSIONS	7-1
8 REFERENCES	8-1

NEDO-24781-1

1 INTRODUCTION

This is an interim data report on the Scaled Multivent Test Program being performed by Creare Incorporated for the General Electric Company and the Mark II Utility Owners' Group. This program will generate a significant single vent and multivent chugging data base (at several scales) for determining and understanding multivent effects. This data base is being generated in two phases along with supporting analyses to demonstrate the applicability of these subscale data. Phase 1 of this test program has been completed and the data from this phase are presented in this report. A final Phase 1/Phase 2 report will be issued upon completion of Phase 2 of this program.

1.1 Background

After the initial pool swell transient during a postulated LOCA in a BWR, steam with decreasing amounts of air is vented from the drywell into the wetwell of the Pressure Suppression System. The purpose of this venting is to condense the steam in the wetwell pool so as to limit the pressure buildup in the containment. During such steam venting, condensation-driven oscillations have been observed in various experiments [1,2].

Two types of condensation-driven oscillations have been observed [1]. The first type, called "condensation oscillations", occur during the earlier portion of the blowdown and are characterized by fairly sinusoidal pressure oscillations in the entire drywell, vent and wetwell system. These condensation oscillations are followed by the second type of condensation-driven oscillations called "chugging". Chugging is characterized by discrete bursts of pressure oscillations in the wetwell pool with quiescent periods between them. The pressure oscillations during chugging are associated with the rapid collapse of the steam "bubble" at the vent exit and typically exhibit a pressure spike followed by a damped ringout which has predominant frequency components at the vent and pool natural frequencies.

An overview of the Mark II chugging program is shown in Figure 1-1. The Mark II Lead Plant Chugging Loads Justification Report [3] provided a technical basis for permitting the licensing review of the lead Mark II plants to proceed in advance of confirmatory analytical and testing efforts. That report demonstrated that design loads were conservatively bounded by the full-scale single-cell loads measured in the 4T facility tests. The Scaled Multivent Test Program was initiated to provide experimental confirmation of the bounding nature of single-cell loads.

Containment loads for assessment of later Mark II plants may be calculated from the improved chugging load definition currently under development in Mark II Task A.16 or by alternate methods. The methods use full-scale single-cell 4T data and extend their application to multivent Mark II plants.

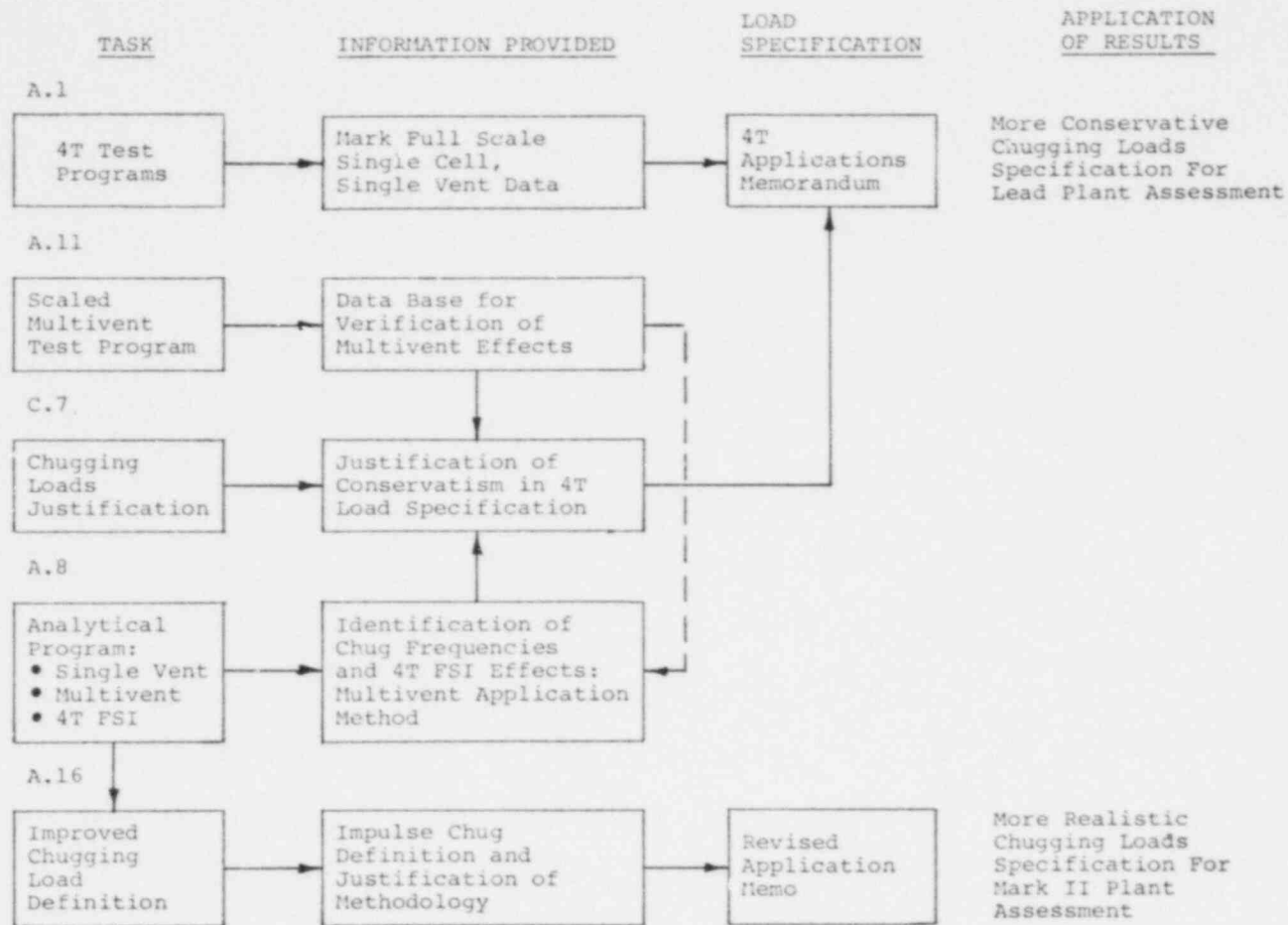


Figure 1-1. MARK II CHUGGING PROGRAMS OVERVIEW

1.2 Scaled Multivalent Test Program Overview

The detailed program plan and description of the Scaled Multivalent Test Program are given in References 4 and 5, and will be briefly summarized here.

The main objectives of the Scaled Multivalent Test Program were to determine multivalent effects on chugging (such as trends in pool wall pressure magnitudes with number of vents), to demonstrate that the multivalent trends observed at subscale remain valid at full scale, and to provide a data base for assessment of analytical load application techniques.

To meet these objectives, tests in single vent geometries at four scales (1/10, 1/6, 1/4 and 5/12 scale), and multivalent geometries at two scales (3, 7 and 19 vents at 1/10 scale and 3 and 7 vents at 1/6 scale) were included in the Scaled Multivalent Test Program. Special tests to determine the effects of drywell volume, pool size and vent location in the pool were also included. The testing was divided into two phases as shown in Figure 1-2. The overall program schedule is shown in Table 1-1.

Phase 1 included the design and construction of the test facility (see Section 2.1), the instrumentation (Section 2.2), and the data acquisition (Section 3.1) and reduction hardware and software (Section 3.2). After a shakedown of the complete facility including instrumentation, data acquisition and reduction systems, Phase 1 tests were performed on the 14 geometries described in Section 2.1. Five of these 14 geometries provided the Phase 1 portion of the baseline single and multivalent test data. These five geometries were the 1, 3 and 7 vent configurations at 1/10 scale and 1 and 3 vent configurations at 1/6 scale.

The remaining geometries tested in Phase 1 provided data on the effects of drywell volume, pool size and vent location in the pool. The test matrices (Section 4) encompassed a wide range of test parameters such as steam mass flux, pool temperature, etc. Over 500 tests were run in Phase 1 including repeat runs. The test data and results are discussed in Sections 5 and 6 for the Phase 1 single and multivalent geometries respectively.

In Phase 2, five additional geometries will be tested as shown in Figure 1-2. The data from these and the Phase 1 tests will provide the data base necessary to meet the objectives of the Scaled Multivalent Test Program. The final report will be issued in the third quarter of 1980.

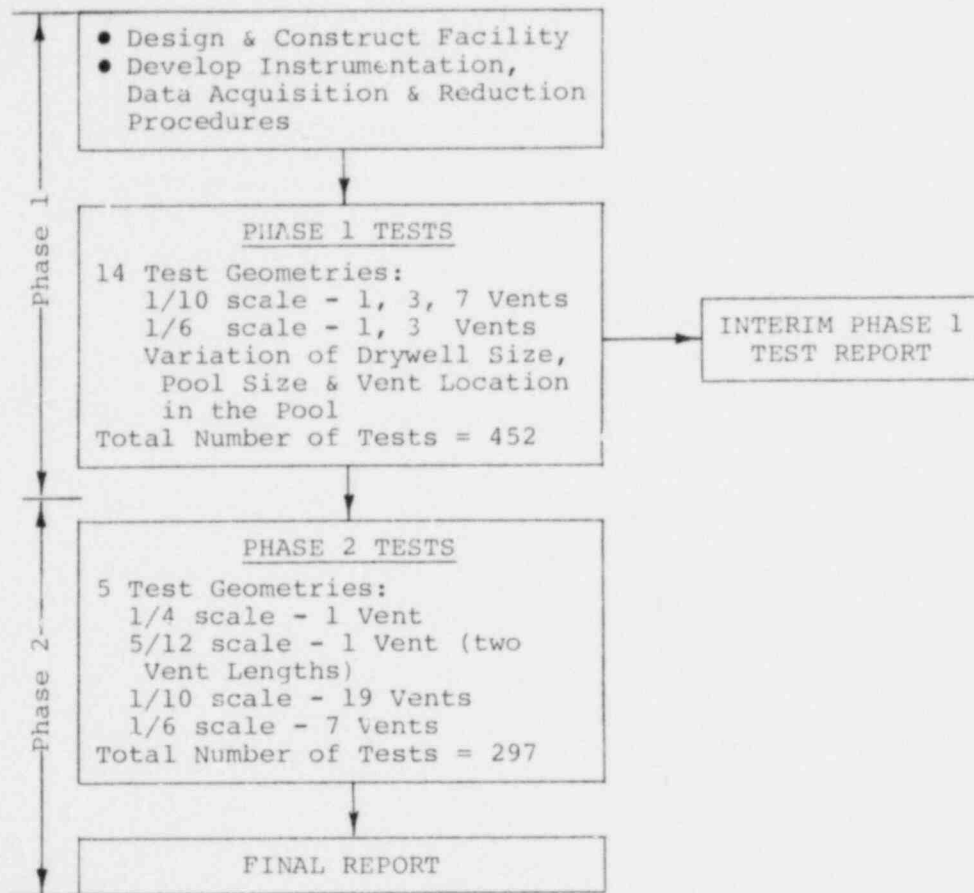


Figure 1-2. SCALED MULTIVENT TEST PROGRAM OVERVIEW

TABLE 1-1 SCHEDULE - SCALED MULTIVENT TEST PROGRAM												
Activity	1978				1979				1980			
	1	2	3	4	1	2	3	4	1	2	3	4
<u>Phase 1</u>												
• Facility Construction & Shakedown	██████████											
• Phase 1 Tests & Analyses				██████████								
• Phase 1 Test Report									▼			
<u>Phase 2</u>												
• Phase 2 Tests						██████████						
• Analyses								██████████				
• Final Report											▼	

2 TEST FACILITY AND INSTRUMENTATION

In this section the test facility, test geometries and instrumentation used in Phase 1 of the Scaled Multivent Test Program are described.

2.1 Test Facility and Geometries

The Scaled Multivent Test Facility is shown schematically in Figure 2-1. It includes a steam supply, a water supply system, an air supply system and the five test vessels used for the single and multiple vent geometries. Of these five test vessels, four were used in Phase 1 of the Multivent Test Program.

Steam was provided from a 20,000 lb/hr, 200 psi boiler with a full flow discharge pressure regulator and flow control valves. The steam flow rate into the drywells was measured with standard orifice meters, with three meters provided for each test geometry to cover the wide range of flows required in the test matrix. One of the meters (in a 4 in. Schedule 40 pipe) was located immediately downstream from the boiler pressure regulator and delivered steam to a header from which the steam was distributed to the geometry under test. During shakedown testing, it was found that the condensation rate in the header could be as high as 0.01 lb/sec. This resulted in the inclusion of two "portable" steam meters (in 2 in. Schedule 40 and 1.0 in. ID pipes) located close to the vessel under test, that draw steam from the header and deliver it to the drywell for low steam flow tests. The portable meters were used when the condensation loss in the header was greater than about 5% of the desired flow rate. Steam condensation between the portable meters and the drywells was estimated to be less than 5% of the lowest steam flow rate for the geometry under test. A constant steam flow was maintained independent of drywell pressure fluctuations by using a choked valve at the steam inlet to the drywell.

Coolant water was supplied to the vessel under test to maintain the desired pool temperature and vent submergence. The coolant water was provided from large storage tanks and a header system which connected to each of the five test vessels through isolation valves. The return coolant was pumped from the vessel through connections approximately 3 in. below the pool surface and was recirculated back to the supply system through a cooling tower.

Air was provided for pressurizing the test vessels and for mixing with steam in the drywells to provide the desired steam air-content. The system was capable of supplying approximately 0.4 lb/sec of air at 90 psig. The flow rate of air delivered to the drywell was measured with turbine meters, with three meters available to cover the full range required. The air flow rate was maintained constant independent of drywell pressure fluctuations by using a choked flow control valve at the inlet to the drywell.

The scaled* geometries tested in Phase 1 are shown in Table 2-1, along with the as-built critical dimensions. The dimensions of the reference Mark II containment from which these test geometries were scaled are shown in Table 2-2. The scale factor is defined as the ratio of the scaled vent diameter to the prototypical vent diameter. The vent submergence and clearance were scaled linearly. The drywell volume was scaled down by the cube of the scale factor and the pool to vent area ratio was

*The scaling rationale is given in Reference 4.

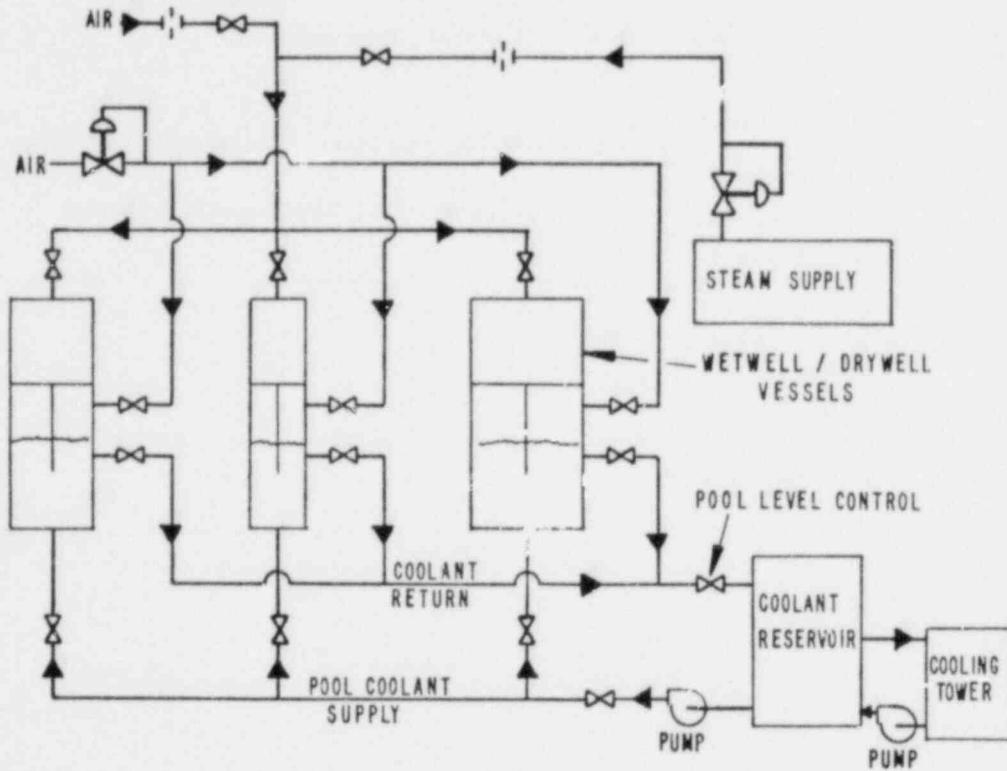


Figure 2-1. SCHEMATIC OF THE SCALED MULTIVALENT TEST FACILITY

TABLE 2-1
 SCALED MULTIVENT TEST PROGRAM
 PHASE I TEST GEOMETRIES

Geometry Code	Geometry Number	Vent Diameter (in.)	Scale	Number of Vents	Vent Length (ft)	Wetwell Diameter (in.)	Drywell Volume (ft ³)	Vent Clearance (in.)	Vent Submergence (in.)	Vent Offset (in.)	Pool To Vent Area Ratio	Test Matrix Type*
A	1	2.32	1/10	1	9.47	10.02	2.5	14	14	0	18.6	I
B	2	2.32	1/10	1	9.47	17.25	2.5	14	14	0	55.3	II
C	3	2.32	1/10	1	9.47	17.25	7.3	14	14	0	55.3	II
D	4	2.32	1/10	1	9.47	17.25	32	14	14	0	55.3	II
E	5	2.32	1/10	1	9.47	17.25	2.5	14	14	4	55.3	II
F	6	2.32	1/10	1	9.47	29.25	2.5	14	14	0	159	II
G	7	2.32	1/10	1	9.47	29.25	2.5	14	14	6	159	II
H	8	2.32	1/10	1	9.47	29.25	2.5	14	14	10	159	II
J	9	3.83	1/6	1	8.72	17.25	11	23	23	0	20.3	I
K	10	2.32	1/10	3	9.47	17.25	7.3	14	14	0	18.4	I
L	11	2.32	1/10	3	9.47	17.25	32	14	14	0	18.4	II
M	12	3.63	1/6	3	8.72	29.25	33	23	23	0	19.5	I
N	13	3.83	1/6	3	8.72	29.25	93	23	23	0	19.5	II
P	14	2.32	1/10	7	9.47	27.25	17.3	14	14	0	19.6	I

* See Section 4.

Parameter	Reference Dimension
Vent Diameter	24 in.
Vent Length	42 ft
Drywell Volume	2655 ft ³ /vent
Vent Clearance	12 ft
Vent Submergence	12 ft
Pool to Vent Area Ratio	19.5

Geometries*	Purpose
A, K, P	Baseline 1/10 scale single vent/multivent data
J, M	Baseline 1/6 scale single vent/multivent data
B, C, D	Effect of drywell volume on single vent chugging (larger drywell volumes used correspond to those used in MV tests)
L, N	Effect of oversized drywell volume on multi-vent chugging
A, B, F	Effect of pool size (centered vent)
B, E	Effect of vent location in 18 in. pool
F, G, H	Effect of vent location in 30 in. pool
A, E, H	Effect of pool size with vent located at the same distance (5 in.) from the 0° circumferential wall location
B, G	Effect of pool size with the vent located at the same distance (9 in.) from the 0° circumferential wall location
* See Table 2-1.	

preserved at the prototypical value except for geometries where it was deliberately varied. Vent lengths were chosen to be approximately 9 ft for all configurations regardless of scale. This length provided the best match to the requirement for multiple use of several test vessels.

The type of data comparisons that can be made using the test data from the Phase 1 test geometries are illustrated in Table 2-3. Geometries A, K, P provided the baseline 1/10 scale 1, 3 and 7 vent data; geometries J and M the baseline 1/6 scale 1 and 3 vent data. Drywell volume effect on single vent chugging was obtained in geometries B, C, and D. Geometries L and N provided the effect of oversized drywell volume on multivent chugging. The data on the effect of pool size and vent location in the pool were obtained in geometries A, B, C, D, E, F, G and H. These data can be used to determine the dynamics of the chug induced pressure waves in the pool and help in understanding the multivent data.

The five baseline geometries having 1, 3 and 7 vents at 1/10 scale and 1 and 3 vents at 1/6 scale are shown schematically in Figures 2-2 and 2-3. The wetwell vessels were fabricated from standard schedule steel pipe of nominal 10 in., 18 in., 28 in., and 30 in. diameter and have 3/8 in. nominal wall thickness. These vessels are capable of operating pressures from 0 to 50 psia. All the test geometries had the drywell mounted on top of the wetwell similar to the Mark II drywell/wetwell configuration.

Vent diameters were chosen at 2.32 in. (2 1/2 in. Schedule 80) and 3.83 in. (4 in. Schedule 80) for the 1/10 and 1/6 scale geometries to optimize vessel use and maintain a constant pool-to-vent area ratio. This area ratio was $19.5 \pm 5\%$ for all of the Phase 1 geometries, except where it was purposely varied to study the effect of pool size.

The layout of the multiple vents in the wetwell pools was designed to produce the following features:

- 1) Constant vent-to-vent spacing for all configurations at a single scale.
- 2) Constant vent-to-wall spacing at some locations on the wall.
- 3) Hexagonal cells that were constant in size for a given scale and whose total area relates in a reasonably constant fashion to pool area.

Figures 2-4 and 2-5 show the single and multiple vent layouts at 1/10 and 1/6 scales. The multivent layouts were constructed by maintaining the size of each hexagonal cell surrounding the vents equal to the hexagonal cell which fits inside the single vent wetwell. The ratio of the total area of the hexagonal cells to the pool area was approximately the same from configuration to configuration. The pool-to-vent area ratios for the 1, 3 and 7 vent configurations at 1/10 scale were 18.6, 18.4 and 19.6 respectively, and the hexagonal cell to pool area fractions were 0.827, 0.837 and 0.783, respectively. For the 1/6 scale 1 and 3 vent configurations, the pool-to-vent area ratios were 20.3 and 19.4 and the hexagonal cell to pool area fractions were 0.827 and 0.863 respectively.

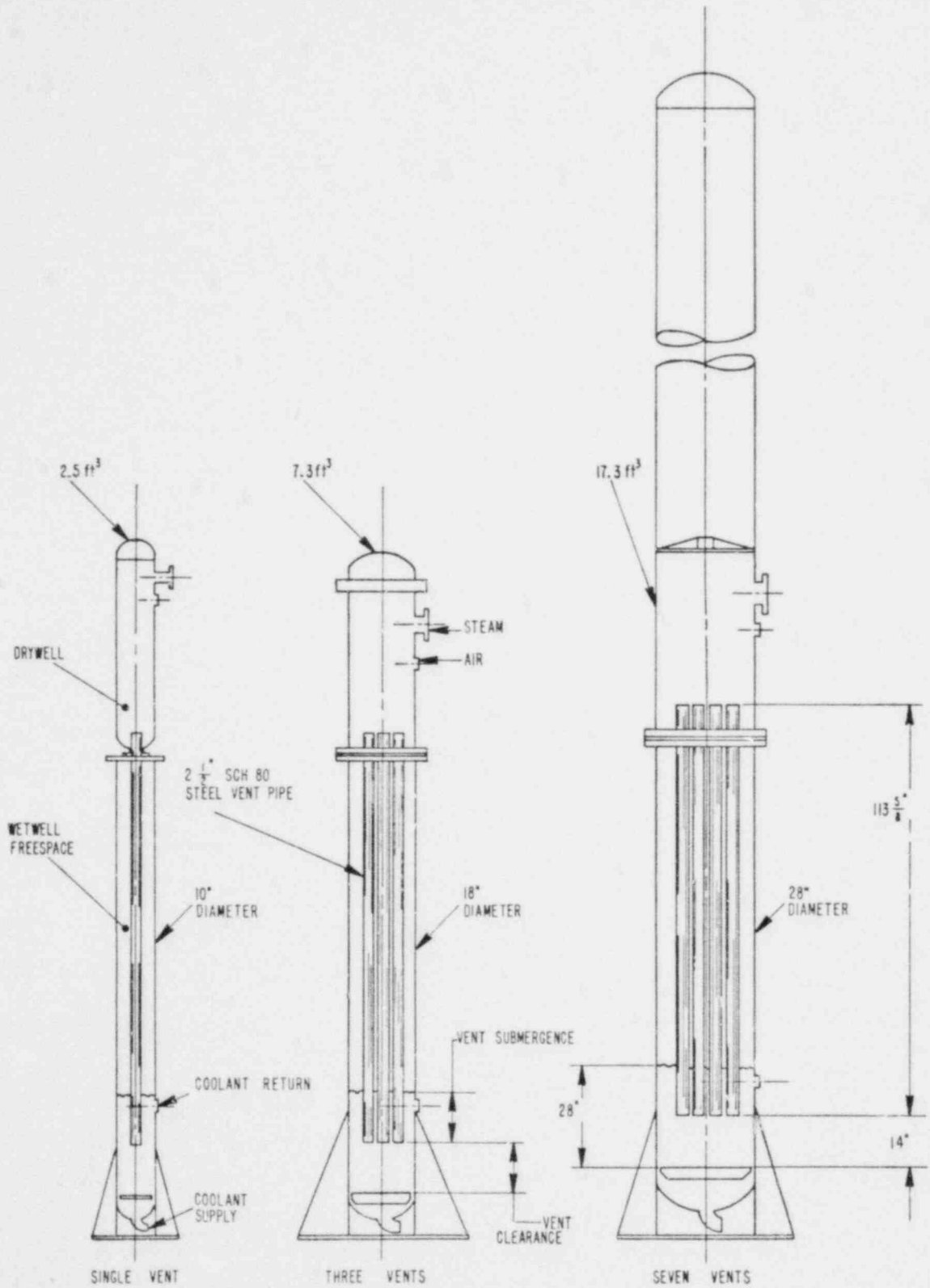


Figure 2-2. SCALED MULTIVENT TEST PROGRAM—PHASE 1 1/10 SCALE BASELINE GEOMETRIES

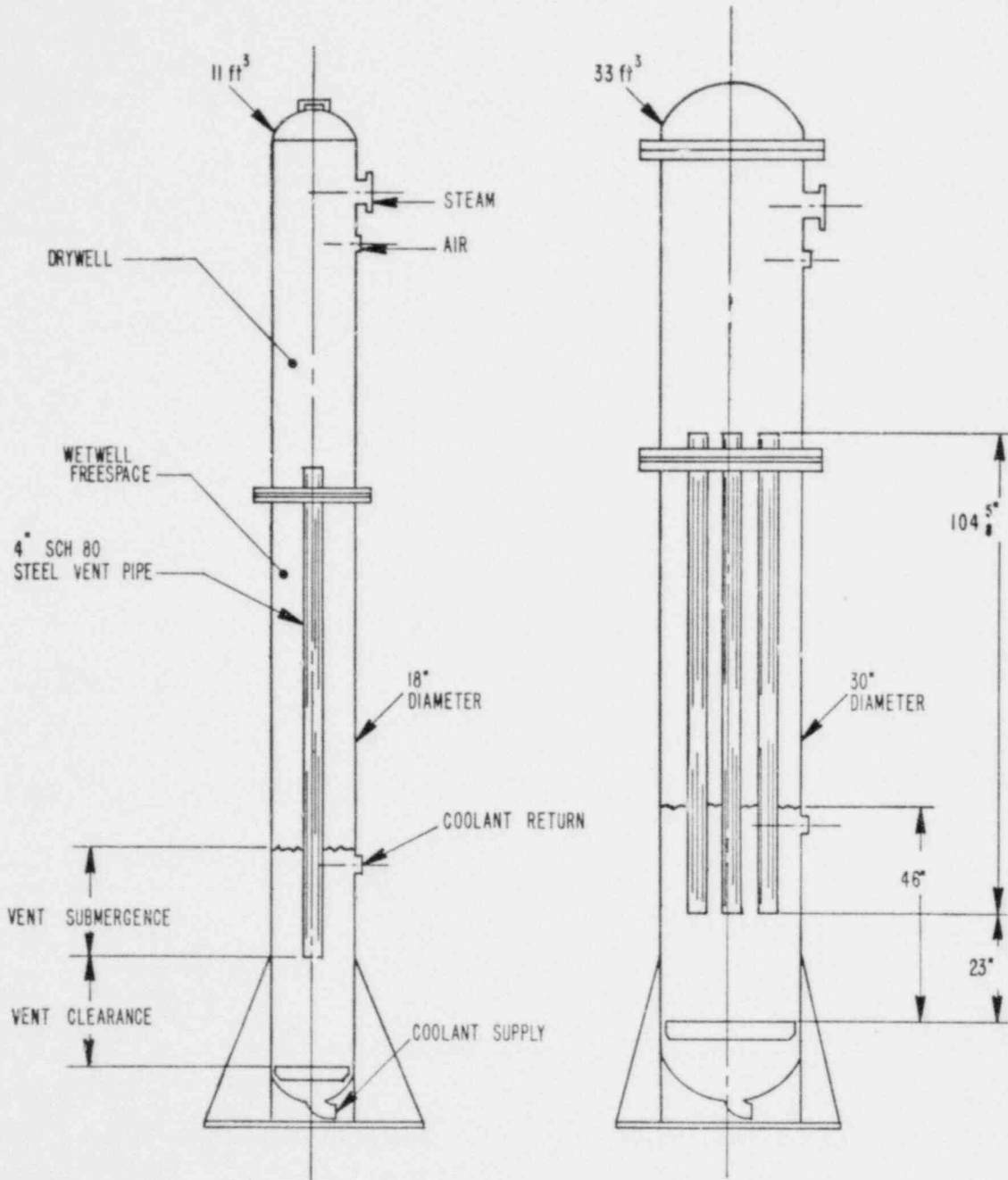
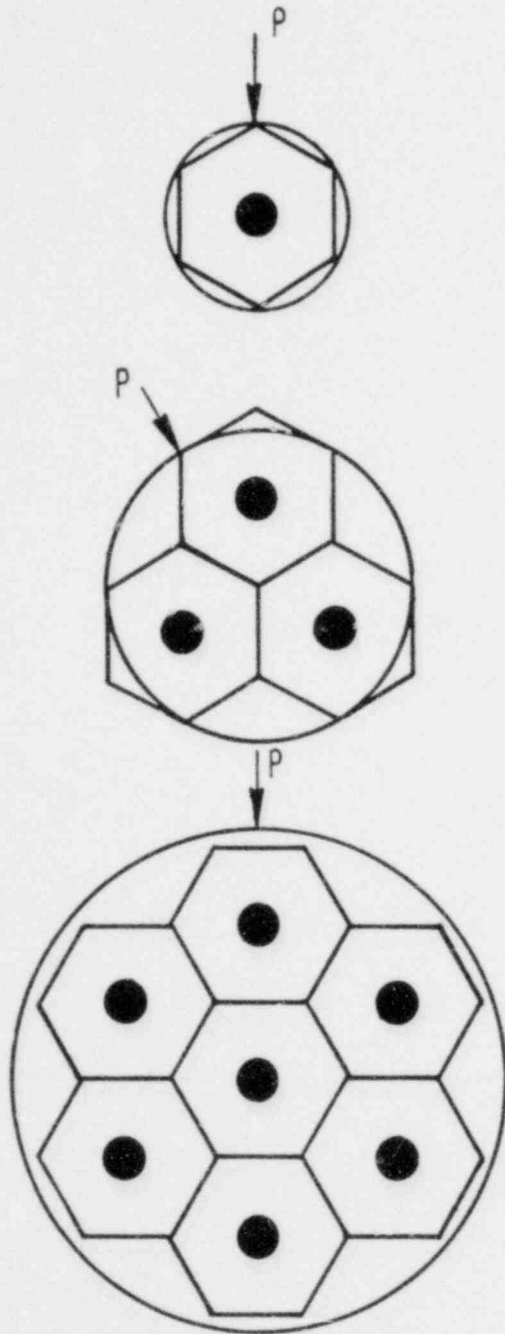


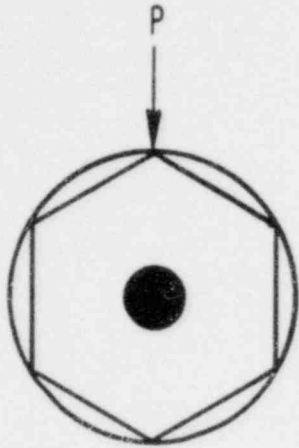
Figure 2-3. SCALED MULTIVENT TEST PROGRAM—PHASE 1 1/6 SCALE
BASELINE GEOMETRIES



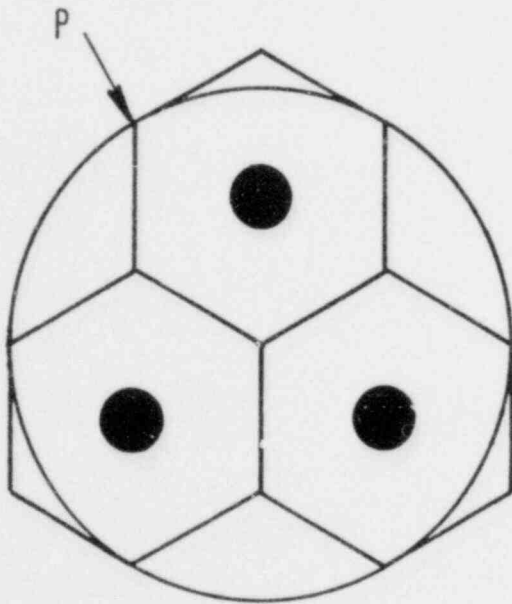
DIMENSIONS	NO. OF VENTS		
	1	3	7
VENT DIAMETER	2.32"	2.32"	2.32"
POOL DIAMETER	10.02"	17.25"	27.25"
POOL TO VENT AREA RATIO	18.6	18.4	19.6
HEXAGONAL CELL TO POOL AREA RATIO	0.827	0.837	0.783

"P" DESIGNATES TYPICAL WALL PRESSURE TRANSDUCER LOCATIONS

Figure 2-4. 1/10 SCALE VENT ARRANGEMENTS



DIMENSIONS	NO. OF VENTS	
	1	3
VENT DIAMETER	3.83"	3.83"
POOL DIAMETER	17.25"	29.25"
POOL TO VENT AREA RATIO	20.3	19.5
HEXAGONAL CELL TO POOL AREA RATIO	0.827	0.863



"P" DESIGNATES TYPICAL WALL PRESSURE TRANSDUCER LOCATIONS

Figure 2-5. 1/6 SCALE VENT ARRANGEMENTS

Vent lengths were chosen to be approximately 9 ft for all configurations regardless of scale. This length provided the best match to the requirement for multiple use of several of the test vessels. All vents extended above the diaphragm plate separating the drywell from the wetwell by 6 to 8 inches. The vents were supported in the wetwell by struts which centered the vent assembly within the pool and provided lateral stiffness. In the case of multiple vent arrays, each vent was also tied to the adjacent vents. These struts were 1/2 in. thick by 3 in. wide steel plate welded to the vent pipes and located 20 in. above the vent exit elevation for the 1/10 scale vents and 24.5 in. for the 1/6 scale vents.

2.2 Test Procedures

Tests in Phase 1 of the Scaled Multivent Test Program were run in a steady-state mode where coolant water was supplied to the wetwell pool to maintain a constant mean pool temperature at a fixed steam mass flux, steam air-content and wetwell airspace pressure. The pool level, and hence vent submergence, was controlled manually by adjusting the coolant return rate. Steam and air were supplied to the drywell through choked flow control valves.

A test was initiated by establishing steady values of the wetwell airspace pressure, steam mass flux, steam air-content, pool temperature and pool level. All of these parameters were monitored by the computer-based data acquisition system and reduced and displayed in real-time to assist the operators in adjusting the test conditions within predetermined tolerances. Following several minutes of steady operation, the main data acquisition sequence was initiated and data were collected for around 100 seconds. At the end of the test, average values of the critical test parameters during the test were printed out from the computer and checked against the desired test conditions.

Under certain conditions it was not possible to maintain a steady pool temperature and the test was run in a transient pool temperature mode. Generally, this occurred at low steam mass fluxes and low subcoolings (high pool temperature) where significant thermal stratification occurred within the pool, and an occasional sharp chug would cause rapid mixing in the pool. For these tests, the coolant flow rate through the pool was set slightly lower than that needed to maintain thermodynamic equilibrium and the data acquisition sequence was initiated when the indicated pool temperature was approximately 10°F below the desired nominal value. During the course of the 100 second data acquisition sequence, the temperature would usually rise to about 10°F above the nominal value.

At some test conditions no chugging occurred (i.e., no appreciable pressure oscillations were observed). This was at a low steam mass flux and high subcooling (cold pool) where steady condensation occurred at the steam/water interface near the vent exit. For these tests, no data were recorded.

2.3 Instrumentation

The Scaled Multivent Test Facility was provided with sufficient instruments to obtain the measurements required to meet the objectives of the test program. These measurements were classified into two main categories, principal and system. The principal data consisted of pool wall pressures,

"source" pressures, pool temperatures, wall and vent accelerations, vent static pressure and vent water level. In addition to pool pressures and temperature distributions, these data were used to determine the phasing between vents and other information to assist in understanding chugging and multivent effects. The system data were data needed to establish the test conditions such as steam and air flow rates to the drywell, drywell pressures and temperatures, vent submergence, and wetwell freespace pressure and temperature. A schematic diagram of the measurement locations is given in Figure 2-6 and the instrument specifications, cross-referenced to Figure 2-6, are given in Table 2-4.

2.3.1 Principal Data

Pool Wall Pressures - Pool wall pressures were measured using flush-mounted, fast response pressure transducers which were protected from thermal transients without loss of frequency response. The pool wall pressures were measured at four horizontal planes in the pool:

- 1 in. above pool bottom elevation.
- Mid-clearance elevation.
- One vent diameter below vent exit elevation at three circumferential positions.
- Mid-submergence elevation.

Pool Temperatures - The pool temperature measurements were made with grounded junction copper-constantan thermocouples having a time constant of less than one second in water. Temperatures in the pool were measured at 12 locations for the single vent geometries and at 13 locations for the multivent geometries. The temperature measurement locations were:

- One thermocouple 3 in. above the pool bottom.
- One thermocouple at the mid-clearance elevation.
- Up to five thermocouples located at one vent diameter below the vent exit. Three thermocouples were mounted on a rake to provide a radial temperature profile. For the single vent geometry only two radial thermocouples were used at this elevation; the innermost thermocouple was eliminated to avoid possible interference with the steam bubble dynamics at the vent exit. Also, at this same elevation, two more thermocouples were located equally spaced around the circumference of the vessel.
- Five thermocouples were located at the vent mid-submergence elevation, three on a radial rake and two more at equally spaced circumferential positions.
- One thermocouple 3 in. below the pool surface elevation.

Vent, Pool Wall and Basemat Accelerations - The accelerations were measured using piezoelectric accelerometers at three locations:

- Accelerometer (up to 3) located on the vent(s), one vent diameter above the vent exit, the sensitive axis lying on a plane perpendicular to the vent pipe axis.
- One accelerometer located on the wall of the vessel at one vent diameter below the vent exit, with the sensitive axis horizontal.
- One accelerometer located on the 1 in. thick vessel support ring which is used to secure the test vessel to the concrete basemat.

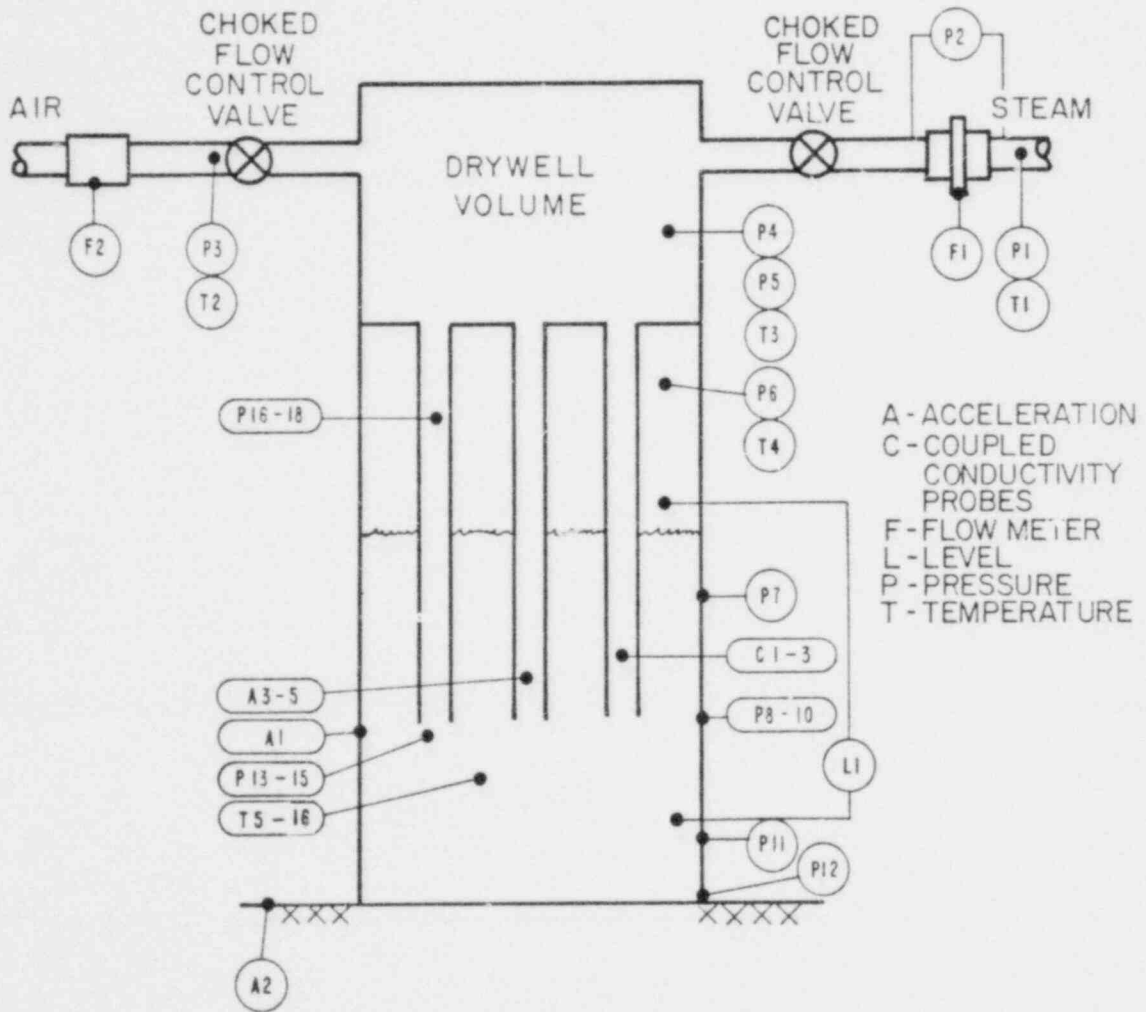


Figure 2-6. SCHEMATIC OF INSTRUMENT LOCATIONS (KEYED TO TABLE 2-4)

TABLE 2-4
INSTRUMENT LIST

Measured Parameter	Identification*	Instrument Type	Instrument Calibration Accuracy	Total Measurement Accuracy	Rise Time	Tolerances On Set Conditions
Steam Supply Pressure	P1	Pressure Gauge and Transducer	± 0.5 psi	± 1.0 psi	—	—
Orifice Meter Differential Pressure	P2	Differential Pressure Transducer	± 0.5 " H ₂ O	± 0.6 " H ₂ O	—	—
Steam Supply Temperature	T1	Thermocouple	$\pm 2^\circ\text{F}$	$\pm 4^\circ\text{F}$	—	—
Steam Flow	F1	Orifice Meter	$\pm 2\%$	$\pm 6\%$	—	$\pm 10\%$
Air Supply Pressure	P3	Pressure Gauge and Transducer	0.5 psi	± 1.0 psi	—	—
Air Supply Temperature	T2	Thermocouple	$\pm 2^\circ\text{F}$	$\pm 4^\circ\text{F}$	—	—
Airflow	F2	Turbine Meters	$\pm 5\%$	$\pm 10\%$	—	$\pm 10\%$
Drywell Average Pressure	P4	Pressure Gauge and Transducer	± 0.5 psi	± 3 psi	—	—
Drywell Instantaneous Pressure	P5	Pressure Transducer	± 0.5 psi	± 1 psi	<2 msec	—
Wetwell Airspace Pressure	P6	Pressure Gauge and Transducer	± 0.5 psi	± 1 psi	—	± 2 psi
Pool Wall Pressure	P7-12	Pressure Transducer	± 0.5 psi	± 1 psi	<50 μ sec	—
"Source" Pressure	P13-15	Pressure Transducer	± 0.5 psi	± 1 psi	<50 μ sec	—
Vent Static Pressures	P16-18	Pressure Transducer	± 0.5 psi	± 1 psi	<50 μ sec	—
Drywell Temperature	T3	Thermocouple	$\pm 4^\circ\text{F}$	$\pm 8^\circ\text{F}$	<10 sec	—
Wetwell Airspace Temperature	T4	Thermocouple	$\pm 4^\circ\text{F}$	$\pm 10^\circ\text{F}$	<10 sec	—
Pool Temperatures	T5-16	Thermocouple	$\pm 4^\circ\text{F}$	$\pm 8^\circ\text{F}$	<1 sec	$\pm 15^\circ\text{F}$
Vent Water Level	C1-3	Coupled Cond. Probes (24 per vent)	—	± 4 "	<2 msec	—
Wetwell Water Level	L1	Differential Pressure Transducer	± 1.5 " H ₂ O	± 3 "	—	± 3 " Average
Pool Wall Acceleration	A1	Accelerometer	$\pm 5\%$	$\pm 10\%$	**	—
Basemat Acceleration	A2	Accelerometer	$\pm 5\%$	$\pm 10\%$	**	—
Vent Accelerometer	A3-5	Accelerometer	$\pm 5\%$	$\pm 10\%$	**	—

*See Figure 2-6.
**Frequency response of 5 kHz.

Chugging "Source" Pressures - Pressures (up to 3) in the pool were measured using fast response pressure transducers having specifications similar to those used for the wall pressure measurements. These transducers were supported with 3/4 in. diameter wands projecting radially into the pool through the walls of the vessels at a point one vent diameter below the exit of the vents. The radial position of these probes was mid-way between the wall and the outside diameter of the vent pipe.

Vent Static Pressures - Vent static pressures were measured in up to three vents with fast response transducers which were mounted flush with the inside surface of the vents and approximately 2 ft above the vent exits. These transducers were protected against thermal transients.

Vent Water Levels - Vent water levels were measured in up to three vents using a coupled conductivity probe system. Twenty-four probes were provided per vent, spaced 3 in. apart along the length of the vent, starting 1 in. above the vent exit.

Drywell Pressure - The fluctuating component of the drywell pressure (caused by the rapid condensation during a chug) was measured with a fast response piezoelectric pressure transducer installed in the drywell wall.

2.3.2 System Data

Wetwell Airspace Measurements - The wetwell airspace pressure was measured with a differential pressure transducer referenced to ambient. A mercury barometer was used to measure the atmospheric pressure and convert gauge pressure to absolute values. The temperature in the airspace was measured with a thermocouple extending approximately 4 in. into the airspace and several feet above the nominal pool surface.

Steam Mass Flow Rate - The steam mass flow rate into the drywell was kept constant by using a choked flow control valve at the drywell vessel. Standard orifice meters were used to measure the steam flow rate into the drywell. These meters were designed in accordance with ASME practice [6]. The steam pressure at the inlet to the meter was measured with a pressure transducer referenced to ambient, and the temperature was measured with a thermocouple installed in the steam line. The pressure drop across the orifice was measured with a differential pressure transducer, using condensate pots to ensure constant static levels on each leg of the transducer.

Pool Temperature - The pool temperature was one of the controlled system parameters and the measurement used to define pool temperature was taken from the thermocouple which was located at vent mid-submergence elevation and several inches from the pool wall (see Section 2.3.1).

Air Mass Flow Rate - Air mass flow rate to the drywell was measured with turbine meters. Three turbine meters were available to cover the range of flow rates required in the test matrix. The pressure and temperature of the air supply to the turbine meters were measured with a pressure transducer and thermocouple, respectively.

Drywell Measurements - In addition to the fluctuating pressure component measured as principal data, the average drywell pressure and temperature were also measured using a pressure transducer and thermocouple.

Vent Submergence - The vent submergence (water depth above the vent exit) was controlled during the tests. Pool level was measured using a differential pressure transducer connected between the wetwell airspace and the pool. The vent submergence was determined from the total pool depth data and measured vent clearance.

In addition to the instruments discussed above, the test operator had various panel meter readouts and pressure gauges available to assist in setting and controlling test conditions. Although data from these indicators were not used in any data reduction procedures, they did provide a check on the operation of the data acquisition system.

2.3.3 Instrument Calibration and Measurement Accuracy

All of the pressure transducers and thermocouples used for principal and system data collection were calibrated in accordance with the schedule and procedures outlined in Reference 7. Table 2-4 displays the calibration accuracy for the major instruments used for principal and system data collection. The column headed "Total Measurement Accuracy" includes the effects of individual instrument calibration accuracy, data acquisition system accuracy and short-term gain stability. The last column in Table 2-4 shows the allowable tolerance band on the average value of the measured or derived parameter over the test duration. If the average of the parameter measured during a test fell outside the tolerance band, the test was generally repeated.

3 DATA ACQUISITION AND REDUCTION PROCEDURES

In this section, data acquisition and reduction procedures are described.

3.1 Data Acquisition System and Procedures

The data acquisition system used for recording the test data is shown in Figure 3-1. The signals from the various instruments were conditioned and amplified to give a +5 volt full scale output. The slow response transducer signals listed in Table 3-1 were routed directly via a 64-channel multiplexer to the A/D converter. The fast response transducers listed in Table 3-2 were recorded on a 28-channel FM tape recorder. The reproduce side of the tape recorder was connected to the multiplexer and an oscillograph. The oscillograph output was used for visual monitoring of the data being recorded on the FM tape recorder.

The signals from the A/D converter were fed via a microcomputer (DEC LP11) to a PDP 11/70 minicomputer. Once the data were on the PDP 11/70 they could then be manipulated and displayed on both video and hardcopy terminals. The low response transducer signals were digitized at a rate of 15 Hz in real time, that is, during the actual test. Key test parameters such as steam mass flux, pool temperature, steam air-content, etc. were processed on-line during the test and displayed in engineering units at the data acquisition station. This allowed real-time monitoring of the key test parameters. At the start of a typical test, the test operator set the required test conditions using an analog panel display of the test conditions. The actual test conditions set were monitored using the above mentioned real-time monitoring capability of the data acquisition system. Once the test parameters were adjusted within specified tolerances, a test was initiated.

At the start of the test, a calibration sequence was followed which, starting from zero volts, input a set of known voltages into the signal conditioning/amplifier systems (input at the same point as the raw transducer signal). Based on this sequence, the computer automatically obtained the zero offsets and gains of all the channels and flagged out any malfunctioning channels. After completion of the calibration sequence, test data were recorded for a duration of about 100 seconds. As mentioned earlier, the slow response signals were digitized and input directly to the PDP 11/70, whereas, the fast response channels were recorded on the FM tape recorder. Selected fast response channels were also digitized in real time from the output side of the tape recorder. At the completion of the data recording, time plots and mean values of the key test parameters for the duration of the test were produced. Time plots of the selected fast response channels were also produced to aid in data checking.

3.2 Data Reduction

As described in the previous section, the signals from the slow response channels (listed in Table 3-1) were digitized and input to the PDP 11/70 minicomputer in real time during a test. These channels were digitized at a rate of 15 Hz per channel. This digitization rate was picked because the frequency response of all the slow response channels was less than 5 Hz.

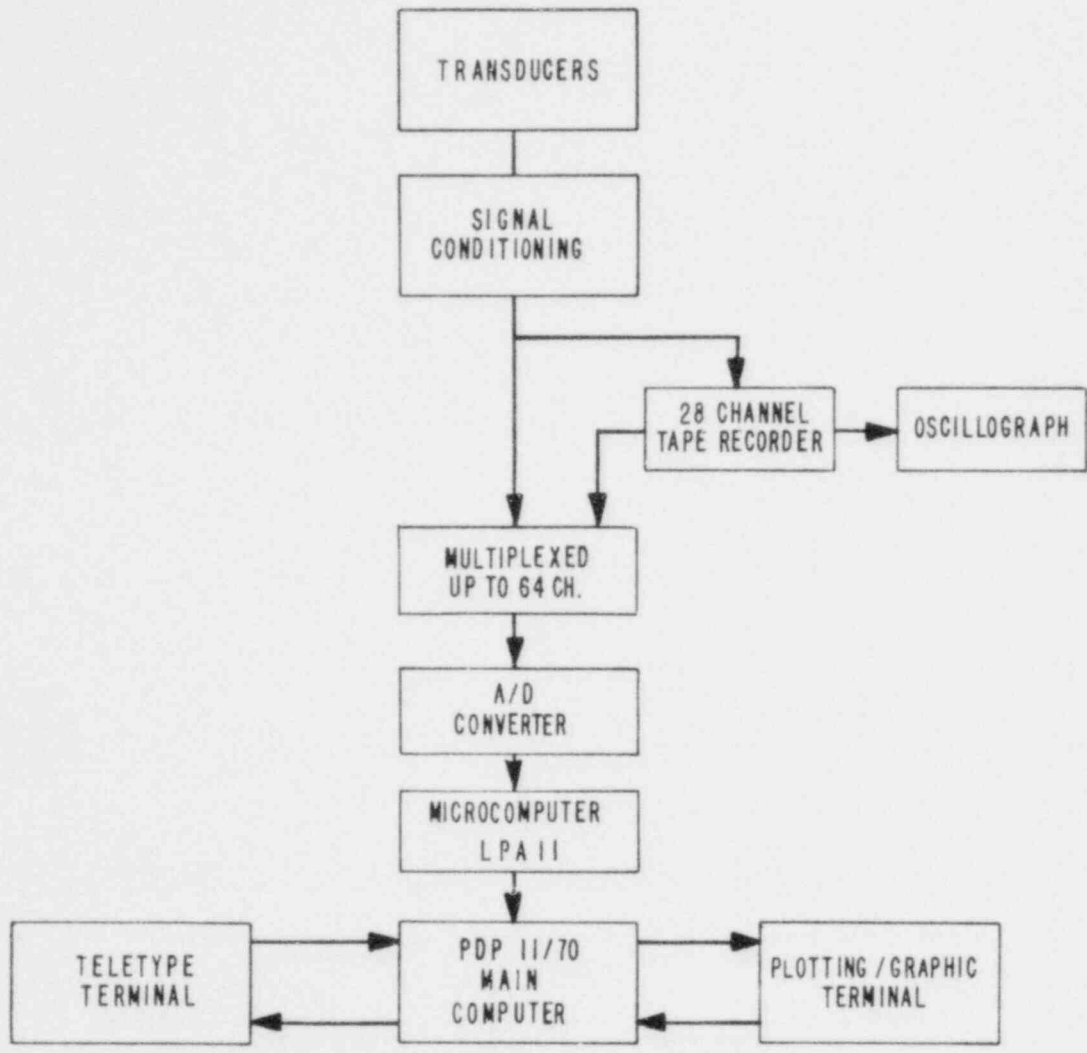


Figure 3-1. SCHEMATIC OF THE DATA ACQUISITION SYSTEM

TABLE 3-1

SLOW RESPONSE CHANNELS* INPUT DIRECTLY TO COMPUTER

	<u>Direct LPA Channel</u>
Air Pressure	28
Wetwell Pressure**	29
Steam Supply Pressure	30
Drywell Pressure	31
Water Flow Rate	34
Steam Flow Rate**	35
Pool Level**	37
Pool Bottom Temperature	38
Mid-Clearance Temperature	39
Exit Elevation 1 Temperature	40
Exit Elevation 2 Temperature	41
Exit Elevation 3 Temperature	42
Exit Elevation 4 Temperature	43
Exit Elevation 5 Temperature	44
Mid-Submergence 1 Temperature	45
Mid-Submergence 2 Temperature	46
Mid-Submergence 4 Temperature	48
Mid-Submergence 5 Temperature	49
Pool Top Temperature	50
Steam Supply 1 Temperature	51
Steam Supply 2 Temperature	52
Remote Steam Supply Temperature	53
Coolant Inflow Temperature	54
Coolant Outflow Temperature	55
Wetwell Outflow Temperature	56
Drywell Outflow Temperature	57
Mid-Submergence 3 Temperature**	58
Remote Steam Flow Rate	59
Remote Steam Pressure	60
Master Reference Voltage	61
Air Flow Rate	62
Air Supply Temperature	63

*Signal conditioning amplifiers band-limited from DC to 3 Hz.

**Also recorded on analog magnetic tape.

TABLE 3-2
FAST RESPONSE CHANNELS* RECORDED ON ANALOG TAPE

<u>Instrument</u>	<u>LPA Channel (from tape reproduce side)</u>	<u>Tape Channel</u>
Bottom Wall Pressure	[0]	16
Vent 1 Static Pressure	[1]	1
Vent 2 Static Pressure	[2]	2
Vent 3 Static Pressure	[3]	3
Vent 1 Source Pressure	[4]	4
Vent 2 Source Pressure	[5]	5
Vent 3 Source Pressure	[6]	6
Vent 1 Wall Pressure	[7]	7
Vent 2 Wall Pressure	[8]	8
Vent 3 Wall Pressure	[9]	9
Mid-Submergence Wall Pressure	[10]	10
Mid-Clearance Wall Pressure	[11]	11
Fast Drywell Pressure	[12]	12
Vent 1 Level	[13]	13
Vent 2 Level	[14]	14
Vent 3 Level	[15]	15
Vent Wall Acceleration	[19]	18
Baseplate Acceleration	[20]	19
Fast Wetwell Pressure	[18]	17
Vent 1 Acceleration	[21]	20
Vent 2 Acceleration	[25]	21
Vent 3 Acceleration	[26]	22
Slow Wetwell Pressure**	[32]	24
Steam Flow Rate**	[33]	25
Pool Level**	[36]	26
Mid-Submergence 3 Temperature**	[47]	27

*Signal conditioning amplifiers band limited from DC to 3 kHz.

**These low response channels also recorded digitally and band limited from DC to 3 Hz.

The data from the slow response channels, which consisted mainly of pool temperatures and system data, were reduced to engineering units and the average values over the test duration were stored for data plotting and display progress.

The fast response channels (listed in Table 3-2), recorded on the FM analog tape recorder, were digitized at a convenient time after the test. The digitization rate for these fast response channels was 10,000 Hz per channel. The fast response channel data were then reduced to give pool wall pressure statistics and vent phasing (for 3-vent multivent tests only). The data reduction procedures used for obtaining these are described below.

3.2.1 Wall Pressure Data Reduction

The wall pressure data were reduced to obtain statistics for the peak overpressures (POP), peak underpressures (PUP) and the period between chugs (t_p). Obtaining these statistics involved locating the individual chugs in a given wall pressure trace and then determining the above-mentioned parameters.

A typical chug wall pressure trace is shown in Figure 3-2. The chug begins with an initial underpressure caused by the rapid condensation and the resulting decrease of the pressure inside the steam bubble at the vent exit. This underpressure is usually followed by an overpressure spike caused by the bubble collapse. The pressure spike is in turn followed by oscillations in the pool wall pressures known as the "ringout". This ringout is the response of the pool and the vent to the bubble collapse process. For many conditions (especially at lower steam fluxes), the ringout decays and wall pressure trace goes back to the zero level before the next chug as shown in Figure 3-2.

A simple algorithm was developed to detect chugs in the pool wall pressure trace and obtain the POP, PUP, and the time at which the POP occurred for each chug. This algorithm works in the following manner. A mean signal level was first computed by averaging the wall pressures over a period τ_a , which was greater than the duration of a chug (see Figure 3-2). A chug was detected when the pressure signal deviated from the mean level by an amount greater than an input threshold—point A in Figure 3-2. Once a chug was detected, the maximum and minimum pressures, i.e., the POP and PUPs within a specified ringout time window τ_r were obtained. The time at which the POP occurred was also recorded. In the case of the chug shown in Figure 3-2, the POP and PUP would correspond to points B and C, respectively. Note that the PUP is not necessarily the initial underpressure preceding the positive pressure spike.

This algorithm had three operator-specified parameters—the averaging period, the threshold value and the ringout time window. The averaging period was selected to be greater than the chug duration and sufficiently long to obtain a good mean signal level. The threshold value was set such that it was 1.5 to 2 times larger than the peak-to-peak value of the noise. The ringout window was chosen by examining the wall pressure trace and determining the time between the initial depressurization and the point where the ringout decayed to below the threshold value.

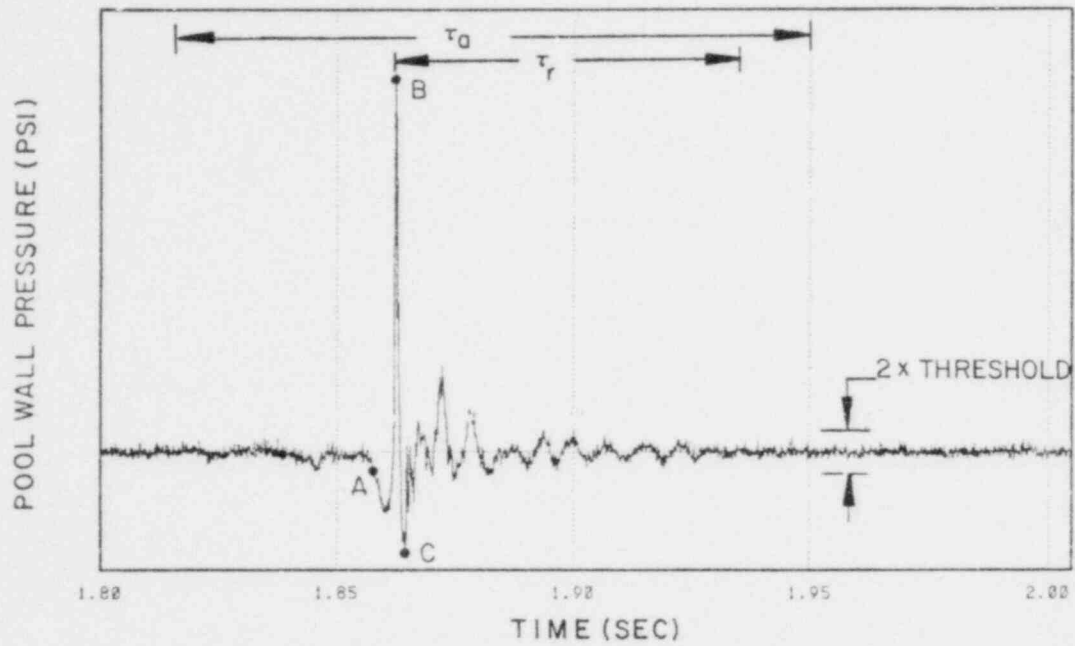


Figure 3-2. TYPICAL TIME WINDOWS AND THRESHOLD USED BY THE CHUG FINDING ALGORITHM

The normal procedure followed in using this algorithm was to first examine the wall pressure trace and choose the three above-mentioned parameters. The algorithm was then run on several seconds of the pressure trace to check (visually on a video terminal) that the values of the parameters chosen did indeed result in the successful detection of all the chugs present in that duration. If the results were positive, the chug finding algorithm was then run for the entire duration of the test or until 300 chugs were detected, whichever occurred first.

This algorithm was only run on the pool bottom elevation pressure trace and the time of occurrence of the POP as well as the magnitude of the POP and PUP for individual chugs were recorded. From these, the mean values and standard deviations for the POP, PUP and period between chugs t_p (time interval between successive POPs) were computed. The cumulative distribution functions were then computed and plotted.

For the other five pool wall pressure traces, POP, PUP and the time of occurrence of the POP were obtained by scanning only those portions of the trace which corresponded to the time window within which a chug was found to occur at the wall bottom location. Using this procedure considerably reduced the time required to process these other pool wall pressure traces.

3.2.2 Vent Phasing Data Reduction

During any single "pool chug"—identified by an oscillation in the pool wall pressure—in a multivent geometry, the phasing information required is:

- at how many vents did bubble collapse occur, i.e., how many vents chugged, and
- what was the delay time between these bubble collapses?

From this, statistical information such as the probability of a given number of vents chugging and the mean delay times between chugs at individual vents during a pool chug can be obtained for a given test condition.

To determine vent phasing, individual vents in the 1/10 scale and 1/6 scale three vent geometries were instrumented with a vent static pressure transducer, coupled conductivity probes and an accelerometer mounted on the vent near the vent exit. After an examination of a large amount of data it was found that the vent static pressure was the best indicator for the occurrence of a chug at a vent.

The pool wall pressure, vent static pressure and vent water level traces for the different types of chugs in the single vent geometry will be discussed below to illustrate the inter-relationship between these traces and how these were used to determine phasing in the multivent geometry.

Figure 3-3 shows the wall pressure and vent static pressure traces and the vent water level trace for a "classical" chug in a single vent geometry. At the start of the chug, the vent is dry and both the pool wall and vent static pressures decrease. This is caused by the rapid condensation occurring at the vent exit which both reduces the pressure in the steam bubble and induces an increased steam flow in the vent which reduces the

This figure is General Electric Company Proprietary and has been removed from this document in its entirety.

Figure 3-3. A CLASSICAL CHUG IN A SINGLE VENT GEOMETRY
(General Electric Company Proprietary)

vent static pressure. The bubble collapse produces the spike in the wall pressure trace. At some point, the condensation at the vent exit is reduced drastically causing a positive pressure wave to propagate up the vent which in turn causes the vent static pressure to increase. From then on, both the pool and vent ring at their respective natural frequencies. Due to the impedance mismatch at the steam water interface, the vent rings at its natural frequency whereas the pool wall pressure ringout contains components from both the pool and vent ringout. For the location chosen for the vent static pressure measurements, it was found that the minimum preceding the maximum in the vent static pressure occurs at about the same time as the positive pressure spike at the pool wall.

The second type of chugs observed is illustrated in Figure 3-4. In these chugs—referred to as "oscillatory" chugs—the pool wall pressure shows periodic pressure oscillations at the same frequency as the oscillations in the vent static pressure. Generally, the vent pressure oscillations for the oscillatory type chugs are smaller in magnitude than those for the classic chugs. Also, for the oscillatory chug, no clear spike is observed in the wall pressure traces.

Other types of chugs observed were combinations of the classic and oscillatory chugs as shown in Figure 3-5 where an oscillatory chug precedes the classical chug. In general, all chugs observed could be placed in one of the three categories described above—classical, oscillatory or a combination of the two. However, for a few tests at the highest steam mass flux of 16 lb/sec ft² and with non-zero steam air-content (see Section 5.3), bursts of periodic pressure oscillations were found to occur which fit in neither of these three categories.

An examination of a large amount of multivent data showed that the chugs occurring at each individual vent in a multivent geometry have similar characteristics as those in a single vent geometry. That is classical chugs, oscillatory chugs and their combinations occur at individual vents (except the ones at 16 lb/sec ft² and non-zero air content). Based on these observations, a phasing algorithm was developed and is described below.

The occurrence of a "pool" chug was detected by using the chug finder on the wall bottom pressure trace. The times at which pool chugs occurred were input to the phasing algorithm. A time window was then defined around the POP for the pool chug which had a total width equal to the sum of the ringout window and half the averaging window chosen for the chug finder algorithm (see Section 3.2.1). This selection for the time window for phasing determination was found to be adequate and consistent with the way the chug finding algorithm picked out pool chugs.

Within this time window for the pool chug, the phasing algorithm scanned the individual vent static pressures to determine if a positive excursion from the mean occurred which exceeded an operator-set threshold. If such an excursion was found, the algorithm then located the preceding minimum in the vent static pressure. Next, the water level probes in that vent were checked to determine if there was any water in the vent. If the water level was below a preset level (generally 1 in.), a classical chug was said to have occurred at that vent. The time of the pressure minimum was then taken to be the time at which the chug occurred at that vent.

This Figure is General Electric Company Proprietary and has been removed from this document in its entirety.

Figure 3-4. AN OSCILLATORY CHUG IN A SINGLE VENT GEOMETRY
(General Electric Company Proprietary)

This figure is General Electric Company Proprietary and has been removed from this document in its entirety.

Figure 3-5. A COMBINATION CHUG—AN OSCILLATORY CHUG PRECEDING
A CLASSICAL CHUG—IN A SINGLE VENT GEOMETRY
(General Electric Company Proprietary)

Once the vent(s) that had classical chugs were identified, the other vent(s) were examined to see if an oscillatory type chug had occurred at these vent(s). The vent static pressures and vent water levels for these vent(s) were examined in a time window of 0.025 sec following the time of occurrence of the first chug found in the pool chug. This 0.025 sec window is slightly greater than the period for the vent quarter wave mode (which was less than 0.020 sec. for the vent lengths used). In this time window, if the vent was found to be dry and the vent static pressure amplitude greater than a second operator-specified threshold, an oscillatory type chug was presumed to have occurred at that vent. (This second vent static pressure threshold was lower than that used for detecting classical chugs since, as mentioned earlier, the magnitude of the pressure oscillations for the oscillatory chugs were smaller than those for the classical chugs). The time of the vent static pressure minimum was taken to be the time of occurrence of the oscillatory chug.

If none of the three vents* were found to have a large positive excursion in the vent static pressure, the phasing algorithm went on to the next pool chug. This means that phasing was determined only for those pool chugs where a classical chug or a combination (classical and oscillatory) chug occurred at one or more vents.

The two threshold values for the vent static pressure mentioned above were set by the operator to give the most reliable phasing data for a given test run. The adequacy of these thresholds was determined by comparison with visual phasing determination for the first 20 pool chugs in the test.

The phasing algorithm was then run on the first 100 pool chugs detected in the test. For each pool chug, the algorithm determined the number of vents that chugged and the time of occurrence of these chugs at the individual vents. From these phasing outputs for individual pool chugs, the percentages of pool chugs with one, two or all three vents chugging were computed. The mean time delay—the time between the first and the last vent to chug in a pool chug—and its standard deviation were also computed. These phasing data were obtained for the 45 psia wetwell airspace pressure tests only. The vent static pressure variations at the lower wetwell airspace pressure were not large enough for adequate phasing determination.

It was recognized from the start of this test program that the determination of phasing would be difficult. Although the phasing algorithm developed performed adequately, it was able to determine phasing for about 70 to 80% of the pool chugs. This should be kept in mind in using the phasing data.

*As mentioned earlier, phasing was determined from the three vent geometries only.

4 TEST MATRIX

The Phase I test matrices are shown in Table 4-1. The Type I test matrix was used for the baseline test geometries—the 1, 3, and 7 vent 1/10 scale geometries and the 1 and 3 vent 1/6 scale geometries. The Type II test matrix was used for the remaining geometries (see Section 2.1).

The test conditions were chosen based on the requirements of the two scaling schemes [4] that were postulated—Froude and Mach scaling. These two scaling schemes result from choosing different sets of parameters to non-dimensionalize the system of equations governing the motion of the steam and water during chugging.

In the Froude scaling scheme, the impetus is to preserve the bubble growth and pool dynamics due to the motion of the steam/water interface in and out of the vent. Froude scaling has been used quite successfully in the scaling of pool swell experiments [8,9]. The main requirements that result from this scaling scheme are:

- system pressure reduced by S ,
- steam mass fluxes reduced by $S^{3/2}$, and
- all dimensions linearly scaled by S ,

where S is the scale factor defined as the ratio of the scaled vent diameter to the full scale vent diameter. The main shortcoming with the Froude scaling scheme is that the thermodynamic parameters affecting condensation cannot be preserved.

The Mach scaling scheme on the other hand, attempts to preserve the condensation process. The condensation phenomenon is mainly governed by the thermodynamic properties (such as subcooling, enthalpies, etc.) of both the liquid and vapor phases. Therefore, the Mach scaling scheme preserves these thermodynamic parameters between scales. The main requirements of this scaling scheme are

- prototypical system pressures,
- prototypical steam mass fluxes,
- prototypical pool temperatures, and
- all dimensions scaled linearly by S .

The test matrices chosen reflect the requirements of the two scaling schemes with tests at reduced wetwell airspace pressure corresponding to Froude scaling, and those at prototypical wetwell airspace pressure (45 psia) corresponding to Mach scaling. Several tests were added at atmospheric wetwell airspace pressure to bridge the gap between the Froude scaled and Mach scaled test conditions.

The important point here is that no single scaling scheme will satisfy all aspects of the chugging phenomenon. Therefore, the test matrices chosen have been made sufficiently broad so as to cover a wide range of test conditions. This coupled with the single vent tests to be performed over a wide range of scales in the Scaled Multivent Test Program will provide sufficient data to evaluate the effects of scale on the chugging phenomenon and demonstrate the applicability of the subscale multivent effects to full scale.

TABLE 4-1a
PHASE 1 TESTS
TYPE I TEST MATRIX FOR GEOMS. 1,9,10,12,14*

Wetwell Airspace Pressure (psia)	4.5 or 7.5		14.7	45	
Steam Mass Flux (lbm/ft ² sec)	0.1,0.2 0.5,1,2	0.1,0.5, 2	0.2,1, 4	0.5,1,2, 4,8,16	1,4, 16
Air Content (%)	0	0.1,0.2, 0.5	0	0	0.1,0.2, 0.5
Temperature (°F)	90,130	90	90,130	90,130 160,200	130
Number of Tests	10	9	6	24	9
Total Number of Type I Tests: 58x5 = 290					

TABLE 4-1b
PHASE 1 TESTS
TYPE II TEST MATRIX FOR GEOMS.
2,3,4,5,6,7,8,11,13*

Wetwell Airspace Pressure (psia)	4.5 or 7.5	45
Steam Mass Flux (lbm/ft ² sec)	0.2,0.5,1	0.5,1,2,4,8,16
Air Content (%)	0	0
Temperature (°F)	90,130	130,160
Number of Tests	6	12
Total Number of Type II Tests: 18x9 = 162		
*See Table 2-1 for test geometry description.		

5 TEST RESULTS AND DISCUSSION—SINGLE VENT DATA AT 1/10 AND 1/6 SCALE

In Phase 1 of the Scaled Multivent Test Program, nine of the 14 geometries tested (see Section 2.1) were single vent geometries. These single vent geometries provided the baseline single vent data at 1/10 and 1/6 scales* and the effects of drywell size, pool size and vent location in the pool. The baseline single vent data are discussed in Sections 5.1 through 5.3 in terms of the effects of the major thermodynamic parameters—steam mass flux, pool temperature and steam air-content—on single vent chugging. The effects of the geometric variations—drywell size, pool size and vent location in the pool are discussed in Sections 5.4, 5.5 and 5.6 respectively.

Only the data at ambient and 45 psia (Mach scaled) wetwell airspace pressure are discussed in the following sections. This is because the Froude scaled data show unclear and in many cases, contradictory trends. A close analysis of these Froude scaled data revealed that both the spike widths and the ringout following the spike vary from geometry to geometry and in many cases from test to test in the same geometry. This indicated that at the Froude scaled conditions, there appeared to be an uncontrolled insurgence of air into the system during the tests due to the subambient system pressures required for these Froude scaled tests. Direct leakage of air into the drywell is unlikely because the test setup was carefully checked for leaks before any tests were performed. The more likely possibility is that air leaked into the system via the coolant circuit or due to deaeration of the coolant water itself caused by the low system pressure. Since air has a very strong effect on the measured pool pressures, the validity of the Froude scaled data is questionable. Therefore, pending resolution of this question regarding air intrusion into the system at the Froude scaled conditions, these data are not presented in this report. Note that air leakage into the system can be entirely ruled out for the ambient and 45 psia wetwell airspace pressure tests and hence the data taken at these conditions (which constitutes the majority of the data taken) are not affected.

Over 170 single vent tests at ambient and 45 psia wetwell airspace pressures were performed in Phase 1. Therefore, to keep the discussion in the following sections concise, data trends are shown using selected representative plots.

The data trends in this section and Section 6 will be presented in terms of the mean values of the peak overpressure (POP), peak underpressure (PUP) and chug frequency (inverse of the mean period between chugs t_p). The mean values are computed from the values of these parameters for individual chugs in a given test. Due to the randomness of chugging, the values of these parameters vary substantially from chug to chug and the standard deviations for these parameters are of the same order as the mean. Typical cumulative distribution functions for the above mentioned parameters are shown in Figure 5-1. From this figure it can be seen that largest spread occurs in the values of the POP, and the maximum POP can be several times larger than the mean value.

*In Phase 2 the single vent data base will be extended to include 1/4 and 5/12 scales. Other subscale data are also available at 1/16 scale [10].

As described in Section 2.3, pool wall pressures were measured at six locations—pool bottom, mid-clearance, vent exit and mid-submergence elevation spaced 120° apart circumferentially. Typical distributions of mean POP at the pool walls are shown in Figures 5-2 and 5-3 for various values of the steam mass flux. These data are for the 1/6 scale single vent geometry. It is seen that the largest mean POP is observed at the pool bottom elevation and decreases with increasing distance from the pool bottom (and theoretically going to zero at the pool surface). This distribution of mean POPs along the pool depth is similar to that expected from acoustic theory for cylindrical pools with the "source" located at the pool center. Also, the magnitudes of the mean POPs at the various locations along the pool depth are related to each other in a nearly constant fashion.

Therefore, although the single vent data trends with the various thermodynamic parameters are presented mainly in terms of the mean POP and PUP at the pool bottom elevation in the following sections, these trends will be the same for the mean POP and PUP at any of the other pool wall locations for a given geometry.

The circumferential distributions of the mean POP at the vent exit elevation are shown in Figure 5-3. It is seen that there is very little circumferential variation in the mean POP as expected for this geometry where the vent is centered in the pool.

In this test program, the control over the test conditions such as steam mass flux, pool temperature etc., was very good and in all cases the test conditions were set well within the specified tolerance bands around the nominal conditions called for in the test matrix. Hence, the repeatability in the reduced data for mean POP, PUP and t_p was quite good. Table 5-1 shows the actual test conditions and the reduced wall pressure data for a set of repeat runs in the 1/10 scale single vent geometry. It is seen that the repeatability is excellent and that the standard deviation of the average values of the wall pressure parameters from the individual tests is small and very close to the measurement uncertainty (± 1 psi) of the pressure transducers used.

TABLE 5-1
TEST REPEATABILITY
(General Electric Company Proprietary)

This table is General Electric Company Proprietary and has been removed from this document in its entirety.

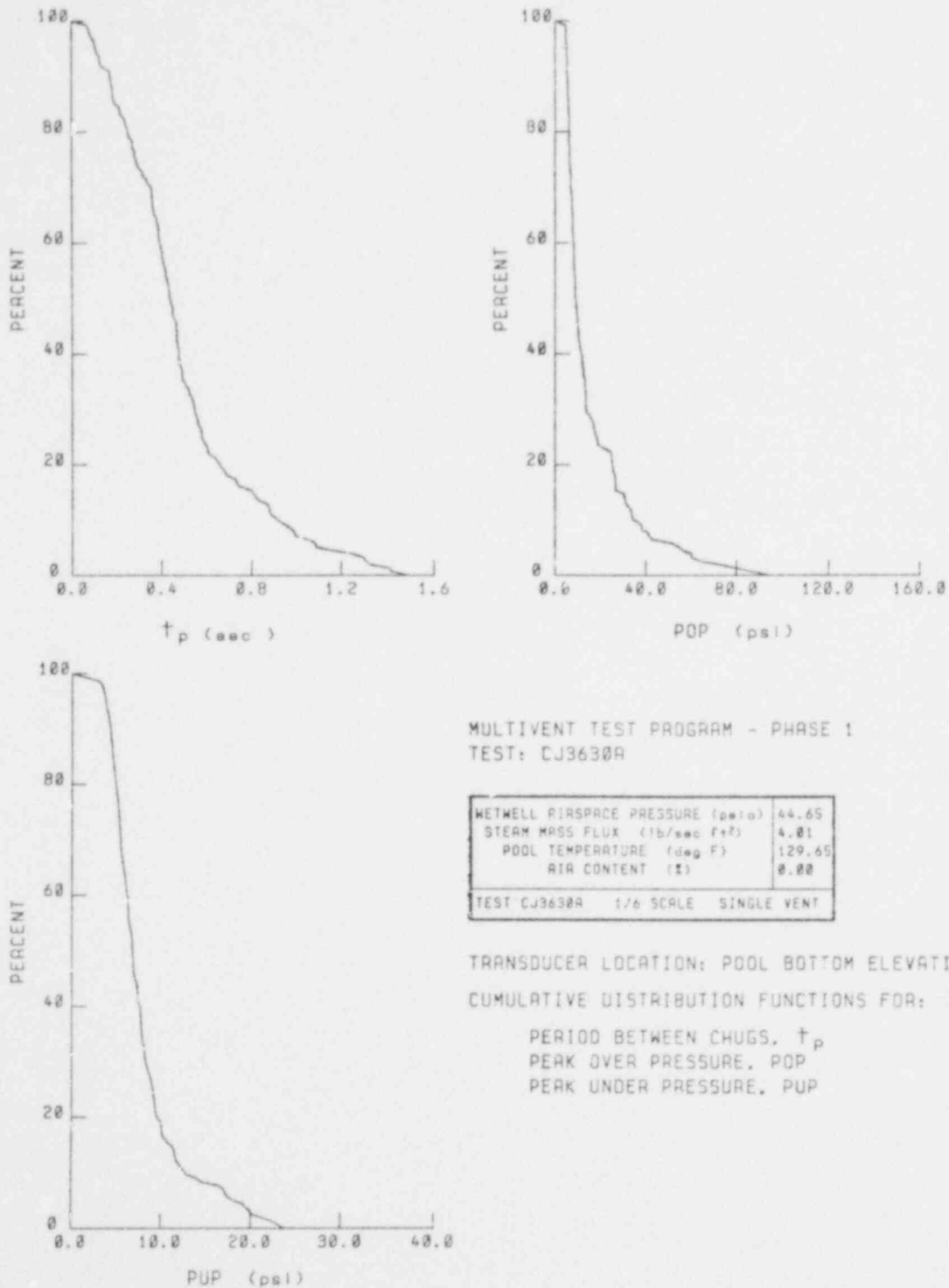


Figure 5-1. TYPICAL CUMULATIVE DISTRIBUTION FUNCTIONS FOR POP, PUP, AND t_p IN A SINGLE VENT TEST

This figure is General Electric Company Proprietary and has been removed from this document in its entirety.

Figure 5-2. POOL WALL PRESSURE DISTRIBUTION—1/6 SCALE SINGLE VENT TESTS (General Electric Company Proprietary)

This figure is General Electric Company Proprietary and has been removed from this document in its entirety.

Figure 5-3. POOL WALL PRESSURE DISTRIBUTION—1/6 SCALE SINGLE VENT TESTS (General Electric Company Proprietary)

5.1 Effect of Steam Mass Flux

In this section, the effect of steam mass flux on single vent wall pressures is described. The steam mass flux is one of the most important parameters affecting chugging loads; it significantly affects both the magnitude and frequency of chugs. Figure 5-4 through 5-9 show traces for the pool bottom elevation wall pressure, vent static pressure, drywell pressure and vent water level from 1/6 scale single vent tests at various steam mass fluxes, 45 psia wetwell airspace pressure, 130°F pool temperature and zero air content. In this set of figures, the scale of the data plots has been maintained constant to permit rapid visual comparison of the pressure and water entry amplitudes.

At the lowest steam mass flux of 0.5 lb/sec ft², chugs are of very small magnitude with no significant fluctuations in the vent static and drywell pressures (Figure 5-4). The vent water level trace shows that the steam/water interface stays near the vent exit (i.e., the vent is dry). From these observations it can be deduced that at this low steam mass flux, steam is condensing at a nearly steady rate at the steam/water interface with occasional bursts of higher condensation rates which cause the interface to wiggle producing the small pressure fluctuations observed at the pool wall.

At a higher steam mass flux of 1 lb/sec ft², the bursts of rapid condensation increase in both frequency and magnitude as indicated by larger pressure oscillations in both the vent static pressure and drywell pressure (Figure 5-5). The magnitude of the chug pressure oscillations at the pool wall is also larger and significant water entry into the vent occurs following a chug. It is interesting to note that rapid condensation also occurs while the steam/water interface is in the vent (around 27.25 sec and 28.9 sec in Figure 5-5). However, such condensation occurring in the vent does not produce any significant pressure oscillations at the pool wall.

At a higher steam mass flux of 2 lb/sec ft², the magnitude of the POP and PUP, the drywell depressurization and the water entry into the vent all increase (Figure 5-6). However, at still higher mass fluxes (Figure 5-7, 5-8, and 5-9), whereas the magnitude of the POP and PUP continue to rise, the drywell depressurization and the water entry into the vent decrease. The magnitude of the vent static pressure fluctuations caused by a chug remains nearly constant. This indicates that the vent flow rate and hence the condensation rate during a chug remains constant in this range of steam mass fluxes.

Also, from these figures it is seen that the period between chugs decreases with increasing values of the steam mass flux. At the highest steam mass flux of 16 lb/sec ft², the chugs follow each other in rapid succession with the pressure oscillations from one chug blending into those of the following chug (see Figure 5-9). The vent static pressure trace at this steam mass flux shows an almost continuous pressure oscillation at the vent acoustic quarter wave frequency of around 48 Hz. The drywell pressure trace also exhibits bursts of very periodic oscillation at about 9 Hz.

Quantitatively, the mean POP, PUP and chug frequency (inverse of mean t_p) as a function of steam mass flux for the same conditions as those for the previous figures are shown in Figures 5-10, 5-11 and 5-12. It is seen that the variations of these parameters with the steam mass flux are consistent with the qualitative observations made above. The mean POP and PUP increase continuously with increasing steam mass flux. The mean chug frequency increases linearly with the steam mass flux. The data for the 1/10 scale single vent are also shown on these figures and the data trends are virtually identical to those for the 1/6 scale data. These data trends are also consistent with those found in previous chugging tests [2,10].

The following Figures are General Electric Company Proprietary and have been removed from this document in their entirety.

<u>Figure</u>	<u>Title</u>	<u>Page</u>
5-4	Data Traces at 0.5 lb/sec ft ² Steam Mass Flux—1/6-Scale Single Vent Test	5-8
5-5	Data Traces at 1.0 lb/sec ft ² Steam Mass Flux—1/6-Scale Single Vent Test	5-9
5-6	Data Traces at 2.0 lb/sec ft ² Steam Mass Flux—1/6-Scale Single Vent Test	5-10
5-7	Data Traces at 4.0 lb/sec ft ² Steam Mass Flux—1/6-Scale Single Vent Test	5-11
5-8	Data Traces at 8.0 lb/sec ft ² Steam Mass Flux—1/6-Scale Single Vent Test	5-12
5-9	Data Traces at 16.0 lb/sec ft ² Steam Mass Flux—1/6 Scale Single Vent Test	5-13
5-10	Variation of Mean POP at Pool Bottom Elevation With Steam Mass Flux—1/10 and 1/6-Scale Single Vent Tests	5-14
5-11	Variation of Mean PUP at Pool Bottom Elevation With Steam Mass Flux—1/10 and 1/6-Scale Single Vent Tests	5-15
5-12	Variation of Mean Chug Frequency With Steam Mass Flux—1/10 and 1/6-Scale Single Vent Tests	5-16

The behavior of the mean POP, PUP and chug frequency with respect to the steam mass flux at other pool temperatures (90°F, 160°F and 200°F) and at ambient wetwell pressure is similar to that described above.

5.2 Effect of Pool Temperature

Pool Temperature Distribution

The pool temperature was defined as the temperature measured by the thermocouple at the mid-submergence elevation and radial location r/D_w of 0.37; where r is the radial distance from the vessel center and D_w is the vessel diameter. For the baseline 1/10 and 1/6 scale single vent geometries, in addition to this thermocouple, there were 11 other thermocouples located in the pool (see Section 2.2) to obtain the pool temperature distribution. The pool temperature distributions in the 1/10 and 1/6 scale geometries for the steam mass fluxes tested at a wetwell pressure of 45 psia and a nominal pool temperature of 130°F are shown in Figures 5-13 through 5-16.

As seen from these figures, the temperature of the pool is quite uniform. The only exception being at the lowest steam mass flux of 0.5 lb/sec ft² where a significant pool thermal stratification occurs along the pool height. At this steam mass flux, the pool temperature remains nearly constant at a value corresponding to the inlet coolant water temperature from the pool bottom up to the vicinity of the vent exit (Figures 5-13 and 5-15). Near the vicinity of the vent exit it rapidly rises to the nominal pool temperature and stays constant at this value up to the pool surface. This stratification occurs because at this low steam flux, no significant chugging occurs and the steam condenses almost steadily with the steam/water interface near the vent exit as described in the previous section. Therefore, very little mixing occurs in the pool. At the higher steam mass fluxes, the chugging causes vigorous mixing in the pool resulting in a uniform pool temperature distribution.

Effects of Pool Temperature

The effect of pool temperature on the mean POP for the 1/10 and 1/6 scale single vent geometries is shown in Figures 5-17 and 5-18. For all steam mass fluxes except 16 lb/sec ft², the mean POP reaches a maximum at a pool temperature between 130°F and 170°F. At 16 lb/sec ft², the mean POP increases continuously with increasing pool temperature over the range of pool temperatures tested. Of course, for all values of the steam mass flux, the mean POP would approach zero as the pool temperature approached the saturation temperature. Therefore, it is expected that at 16 lb/sec ft² steam flux a maximum in the mean POP will occur between pool temperatures of 200°F and 275°F (saturation temperature at the wetwell pressure of 45 psia).

Figures 5-19 and 5-20 show the effect of pool temperature on the mean PUP. It is seen that in general, the mean PUP decreases with increasing pool temperature for steam mass fluxes up to 8 lb/sec ft². At the highest steam mass flux of 16 lb/sec ft² pool temperature has no significant effect on mean PUP over the pool temperature range tested. It is expected that mean PUP would approach zero as the pool temperature approaches the saturation value.

The pool temperature has no significant effect on the chug frequency for steam mass fluxes of 4 lb/sec ft² and lower, as shown in Figures 5-21 and 5-22. At the higher steam mass fluxes, the chug frequency reaches a maximum for a pool temperature between 130°F and 170°F, after which it decreases as the pool temperature is increased further.

The traces for the pool bottom elevation wall pressure, vent static pressure, drywell pressure and the vent water level at 4 lb/sec ft² steam mass flux and various pool temperatures for the 1/6 scale single vent geometry are shown in Figures 5-23 through 5-26. It is seen that the magnitude of the chugs at the pool bottom is the largest for the pool temperatures of 130°F and 160°F (Figures 5-24 and 5-25, respectively). The magnitude of the chugs is lower at both the lowest and highest pool temperatures of 90°F and 200°F. This is consistent with the trends in mean POP shown in Figure 5-18 for this steam mass flux.

Also, at the lowest pool temperature of 90°F (Figure 5-23), the vent static pressure shows almost continuous oscillations, and no large depressurizations are observed in the drywell. Also, condensation of steam occurs when the water is in the vent. At higher pool temperatures, larger drywell depressurizations are observed which correspond to bursts of vent static pressure oscillations indicating that the condensation becomes more intermittent. These larger drywell depressurizations are accompanied by larger water excursions into the vent.

The corresponding traces for the steam mass flux of 16 lb/sec ft² are shown in Figures 5-27 through 5-30. The magnitude of the chugs increases continuously with increasing pool temperatures which is consistent with the trend in mean POP with pool temperature at this mass flux as shown in Figure 5-18. Again, the drywell depressurizations are quite small at the lowest pool temperature of 90°F (Figure 5-24) indicating a more continuous condensation than at higher pool temperatures. The increase in the magnitude of the drywell depressurizations with increasing pool temperatures indicates that condensation becomes more intermittent and the amount of steam condensed in each condensation event increases with increasing pool temperatures.

In summary, the mean POP reaches a peak value at some value of the pool temperature, and the mean PUP decreases with increasing pool temperatures. It is expected that both mean POP and PUP will go to zero as the pool temperature approaches the saturation temperature corresponding to the wetwell airspace pressure. Finally, the chug frequency is not affected by the pool temperature at steam mass fluxes ≤ 4 lb/sec ft². At higher steam mass fluxes, the chug frequency reaches a maximum at some value of the pool temperature after which it decreases with further increase in the pool temperature. These data trends with pool temperature are consistent with those observed in previous chugging tests [2,10].

The following Figures are General Electric Company Proprietary and have been removed from this document in their entirety.

<u>Figure</u>	<u>Title</u>	<u>Page</u>
5-13	Pool Temperature Distributions at Various Steam Mass Fluxes— 1/10-Scale Single Vent Tests	5-19
5-14	Pool Temperature Distributions at Various Steam Mass Fluxes— 1/10-Scale Single Vent Tests	5-20
5-15	Pool Temperature Distributions at Various Steam Mass Fluxes— 1/6-Scale Single Vent Tests	5-21
5-16	Pool Temperature Distributions at Various Steam Mass Fluxes— 1/6-Scale Single Vent Tests	5-22
5-17	Variation of Mean POP at Pool Bottom Elevation With Pool Temperature—1/10-Scale Single Vent Tests	5-23
5-18	Variation of Mean POP at Pool Bottom Elevation With Pool Temperature—1/6-Scale Single Vent Tests	5-24
5-19	Variation of Mean PUP at Pool Bottom Elevation With Pool Temperature—1/10-Scale Single Vent Tests	5-25
5-20	Variation of Mean PUP at Pool Bottom Elevation With Pool Temperature—1/6-Scale Single Vent Tests	5-26
5-21	Variation of Mean Chug Frequency With Pool Temperature— 1/10-Scale Single Vent Tests	5-27
5-22	Variation of Mean Chug Frequency With Pool Temperature— 1/6-Scale Single Vent Tests	5-28
5-23	Data Traces at 90°F Pool Temperature and 4 lb/sec ft ² Steam Mass Flux—1/6-Scale Single Vent Test	5-29
5-24	Data Traces at 130°F Pool Temperature and 4 lb/sec ft ² Steam Mass Flux—1/6-Scale Single Vent Test	5-30
5-25	Data Traces at 160°F Pool Temperature and 4 lb/sec ft ² Steam Mass Flux—1/6-Scale Single Vent Test	5-31
5-26	Data Traces at 200°F Pool Temperature and 4 lb/sec ft ² Steam Mass Flux—1/6-Scale Single Vent Test	5-32
5-27	Data Traces at 90°F Pool Temperature and 16 lb/sec ft ² Steam Mass Flux—1/6-Scale Single Vent Test	5-33
5-28	Data Traces at 130°F and 16 lb/sec ft ² Steam Mass Flux— 1/6-Scale Single Vent Test	5-34
5-29	Data Traces at 160°F and 16 lb/sec ft ² Steam Mass Flux— 1/6-Scale Single Vent Test	5-35
5-30	Data Traces at 200°F and 16 lb/sec ft ² Steam Mass Flux— 1/6-Scale Single Vent Test	5-36

5.3 Effect of Air

The effect of air in the steam was investigated by adding controlled amounts of air to the steam in the drywell.

The air-content of the steam from the boiler was reduced to below 20 ppm by preheating the boiler feedwater to 190°F in an ambient pressure feedwater tank.

The effect of air on the mean POP is shown in Figures 5-31 and 5-32 for the 1/10 scale and 1/6 scale single vent geometries respectively. It is seen that the mean POP decreases with increasing steam air-content. The drop in the mean POP with steam air-content is most pronounced at the steam mass flux of 16 lb/sec ft² where 0.1% steam air-content reduces the mean POP by a factor of about 2.

To determine the sensitivity of the mean POP to very small amounts of air, several additional tests were done in the 1/6 scale single vent geometry at a steam mass flux of 4 lb/sec ft². For these additional tests, steam air-content of 0.01%, 0.05%, and 0.07% were used. These data are included in Figure 5-32. It is seen that such small amounts of air do not affect the mean POP appreciably for this steam mass flux. Note that the smallest value of air-content tested (0.01% or 100 ppm) is much greater than the expected air-content (<20 ppm) of the "pure" steam (i.e., with no air addition). Therefore, small variations in the air-content of the "pure" steam from the boiler will not affect the mean POP by any measureable amount.

The effect of steam air-content on the mean PUP is shown in Figures 5-33 and 5-34. Again, the mean PUP decreases with increasing air-content. This reduction in both the mean POP and PUP with increasing steam air-content indicates that air both reduces the steam condensation rate and "cushions" the bubble collapse.

From Figures 5-35 and 5-36, it is seen that the steam air-content has no appreciable effect on the mean chug frequency except at the highest steam mass flux of 16 lb/sec ft². At this steam mass flux, the chug frequency decreases slightly with increasing steam air-content.

The traces for the pool bottom elevation pressure, vent static pressure, drywell pressure and vent water level at a steam mass flux of 4 lb/sec ft² and various steam air-contents for the 1/6 scale single vent geometry are shown in Figures 5-37 through 5-40. The most noticeable effect of air is seen on the pool wall pressure. In addition to the decrease in the POP and PUP, the pressure spikes are less sharp and the frequency of the ringout following the spike is lower. Also, with increasing air content, chugs with periodic pressure oscillations at the vent harmonic (oscillatory chugs) occur more frequently.

The corresponding traces at the steam mass flux of 16 lb/sec ft² are shown in Figures 5-41 through 5-44. The effect of air on the wall pressure is quite significant. Not only does air reduce the magnitude of the pressure oscillations, but it also modifies the frequency content drastically producing bursts of periodic oscillations.

In summary, both the mean POP and PUP decrease with increasing air content. Further, air reduces the sharpness of chug pressure spike and lowers the frequency of the ringout that follows. Finally, air causes chugs with pressure oscillations at the vent harmonic to occur more frequently. Again, the effects of air on chugging observed here are similar to those in previous chugging tests [2,10].

The following Figures are General Electric Company Proprietary and have been removed from this document in their entirety.

<u>Figure</u>	<u>Title</u>	<u>Page</u>
5-31	Variation of Mean POP at Pool Bottom Elevation With Steam Air-Content--1/10-Scale Single Vent Tests	5-39
5-32	Variation of Mean POP at Pool Bottom Elevation With Steam Air-Content--1/6-Scale Single Vent Tests	5-40
5-33	Variation of Mean PUP at Pool Bottom Elevation With Steam Air-Content--1/10-Scale Single Vent Tests	5-41
5-34	Variation of Mean PUP at Pool Bottom Elevation With Steam Air-Content--1/6-Scale Single Vent Tests	5-42
5-35	Variation of Mean Chug Frequency With Steam Air-Content--1/10-Scale Single Vent Tests	5-43
5-36	Variation of Mean Chug Frequency With Steam Air-Content--1/6-Scale Single Vent Tests	5-44
5-37	Data Traces at 0% Steam Air-Content and 4 lb/sec ft ² Steam Mass Flux--1/6-Scale Single Vent Tests	5-45
5-38	Data Traces at 0.1% Steam Air-Content and 4 lb/sec ft ² Steam Mass Flux--1/6-Scale Single Vent Test	5-46
5-39	Data Traces at 0.2% Steam Air-Content and 4 lb/sec ft ² Steam Mass Flux--1/6-Scale Single Vent Test	5-47
5-40	Data Traces at 0.5% Steam Air-Content and 4 lb/sec ft ² Steam Mass Flux--1/6-Scale Single Vent Test	5-48
5-41	Data Traces at 0% Steam Air-Content and 16 lb/sec ft ² Steam Mass Flux--1/6-Scale Single Vent Test	5-49
5-42	Data Traces at 0.1% Steam Air-Content and 16 lb/sec ft ² Steam Mass Flux--1/6-Scale Single Vent Test	5-50
5-43	Data Traces at 0.2% Steam Air-Content and 16 lb/sec ft ² Steam Mass Flux--1/6-Scale Single Vent Test	5-51
5-44	Data Traces at 0.5% Steam Air-Content and 16 lb/sec ft ² Steam Mass Flux--1/6-Scale Single Vent Test	5-52

5.4 Effect of Drywell Volume

The drywell volume in a baseline multivent test is larger than that in the corresponding single vent test by a factor equal to the number of vents in the multivent geometry. Thus, if the vents chug out-of-phase in the multivent geometry, each vent in effect sees the whole drywell volume. Therefore, a series of tests were performed in Phase 1 to evaluate the effect of drywell volume on single vent chugging. The drywell volume was varied in the geometry with the 1/10 scale single vent in the 18 in. diameter pool (the pool used for three 1/10 scale vents). The drywell volumes used were 2.5 ft³ (1/10 scale single vent drywell), 7.2 ft³, (1/10 scale 3 vent drywell) and 32 ft³.

The effect of drywell volume on the mean POP, PUP and chug frequency is shown in Figures 5-45, 5-46, and 5-47 respectively. From these figures it is evident that the drywell volume has a small effect on the mean POP and PUP, with both the mean POP and PUP decreasing slightly for the largest drywell volume of 32 ft³. The mean chug frequency is independent of drywell volume as seen in Figure 5-47.

Therefore, it can be concluded that any significant differences observed in the mean POP, PUP and chug frequency between single and multivent geometries cannot be attributed to the larger drywell volume the individual vents would see if the vents chug out-of-phase in the multivent geometry.

The following Figures are General Electric Company Proprietary and have been removed from this document in their entirety.

<u>Figure</u>	<u>Title</u>	<u>Page</u>
5-45	Variation of Mean POP at Pool Bottom Elevation With Drywell Volume—1/10-Scale Single Vent Tests	5-54
5-46	Variation of Mean PUP at Pool Bottom Elevation With Drywell Volume—1/10-Scale Single Vent Tests	5-55
5-47	Variation of Mean Chug Frequency With Drywell Volume—1/10-Scale Single Vent Tests	5-56

5.5 Effect of Pool Size

In a multivent geometry, if the vents chug out-of-phase, the individual vents are in effect chugging in a larger pool. Therefore, a series of Phase 1 tests were run to determine the effect of pool size on single vent chugging (see Table 2-1). A 1/10 scale single vent was tested in the 18 in. diameter pool (the 1/10 scale 3 vent pool) and the 30 in. diameter pool in addition to the 10 in. diameter pool (1/10 scale single vent pool).

The variations of the mean POP with wetwell diameter at pool temperatures of 130°F and 160°F are shown in Figures 5-48 and 5-49, respectively. It is seen that the mean POP decreases quite rapidly with increasing pool size. Figures 5-50 and 5-51 show the mean POPs normalized by the respective mean POPs for the 10 in. diameter pool at the two pool temperatures. Also shown on these figures are the lines corresponding to the attenuations proportional to the ratios of the pool diameters and the pool areas. It is seen that the mean POP is approximately inversely proportional to the pool area.

The variations of the mean PUP with pool size for the same two pool temperatures are shown in Figures 5-52 and 5-53. It is seen that the mean PUP also decreases with increasing pool size. The decrease in mean PUP at the higher steam mass fluxes appears to be proportional to the inverse of the pool diameter as compared to the quadratic decrease in mean POP.

The effect of pool size on the chug frequency is shown in Figures 5-54 and 5-55 for pool temperatures of 130°F and 160°F respectively. Increase in pool size increases the chug frequency slightly for most steam mass fluxes.

The decrease of both the mean POP and PUP with increasing pool size implies that if the vents chug out-of-phase in a multivent geometry, the wall pressure will be lower in the multivent geometry as compared with those in the single vent geometry due to the larger multivent pool. This finding is the principal explanation for the multivent multiplier behavior presented in Section 6.

The following Figures are General Electric Company Proprietary and have been removed from this document in their entirety.

<u>Figure</u>	<u>Title</u>	<u>Page</u>
5-48	Variation of Mean POP at Pool Bottom Elevation With Wetwell Size (130°F Pool Temperature)—1/10-Scale Single Vent Tests	5-58
5-49	Variation of Mean POP at Pool Bottom Elevation With Wetwell Size (160°F Pool Temperature)—1/10-Scale Single Vent Tests	5-59
5-50	Variation of Mean POP at Pool Bottom Elevation (Normalized By Mean POP in 10 in. Wetwell) With Wetwell Size (130°F Pool Temperature)—1/10-Scale Single Vent Tests	5-60
5-51	Variation of Mean POP at Pool Bottom Elevation (Normalized by Mean POP in 10 in. Wetwell) With Wetwell Size (160°F Pool Temperature)—1/10-Scale Single Vent Tests	5-61
5-52	Variation of Mean PUP at Pool Bottom Elevation With Wetwell Size (130°F Pool Temperature)—1/10-Scale Single Vent Tests	5-62
5-53	Variation of Mean PUP at Pool Bottom Elevation With Wetwell Size (160°F Pool Temperature)—1/10-Scale Single Vent Tests	5-63
5-54	Variation of Mean Chug Frequency With Wetwell Size (130°F Pool Temperature)—1/10-Scale Single Vent Data	5-64
5-55	Variation of Mean Chug Frequency With Wetwell Size (160°F Pool Temperature)—1/10-Scale Single Vent Data	5-65

5.6 Effect of Vent Offset

The offset vent tests were done to provide data which would help in understanding the mechanics of propagation of the chug-induced pressure waves in the pool and in the understanding of multivent effects. Varying the location of the vent exit (which is the "source" of the chug) will cause variations in the magnitude (mean POP for example) of the pressure signals measured at fixed pool wall locations. By comparing these relative changes in the magnitudes of the pressure at a given location, as well as the pressure distribution in the pool due to the changes in the vent location, insights can be obtained regarding the mechanics of chug-induced wave propagation in the pool. At present, detailed comparisons of data with predictions from analytical models for the pool have not been done. Therefore, in this section the experimental data are presented with few attempts to draw conclusions regarding the wave propagation mechanisms.

In these tests, the vent was offset such that it moves closer to the pressure transducers located at the 0° circumferential location as shown schematically in Figure 5-56. Note that the pressure transducers at the pool bottom, mid-clearance, vent exit and mid-submergence were all located at the 0° circumferential location. Therefore, offsetting the vent moves it closer to all these transducer locations. There were two additional pressure transducers located on the pool walls at the 120° and 240° locations at the vent exit elevation and offsetting the vent moves its exit away from these transducers.

The vent offset tests were done in the geometries with the 1/10 scale vent in the 18 in. and 30 in. diameter wetwells (Table 2-1). The vent offset tested in the 18 in. diameter wetwell was 4 in. For this offset, the distance between the vent center and the transducers located at the 0° circumferential position was the same as that for the 1/10 scale vent centered in the 10 in. diameter wetwell (i.e., the 1/10-scale geometry). Similarly, the vent offsets of 6 in. and 10 in. tested in the 30 in. diameter wetwell also resulted in the same distances between the vent center and the 0° circumferential transducer locations as those for the 1/10 scale vent centered in the 10 in. and 18 in. diameter wetwells, respectively. These offset vent geometries and the corresponding centered vent geometries are shown schematically in Figure 5-57. Also available for comparison is the geometry with the 1/10-scale vent centered in the 30 in. diameter pool.

The effect of vent offset on the mean POP at the vent exit elevation 0° circumferential location is shown in Figure 5-58, where all tests shown in this figure were in the 30 in. diameter pool. As expected, the magnitude of the mean POP at this location increases as the offset is increased and hence the vent to transducer spacing is reduced. (The distance between the vent center and the vent exit elevation transducer at the 0° circumferential location is the difference between the pool radius and the vent offset.) Also shown on Figure 5-58 are lines along which the mean POP is inversely proportional to the distance between the center of the vent and the transducer location. The close agreement between the dashed lines and the data trends indicates that the mean POP does indeed vary as the inverse of the distance between the vent center and the transducer location.

The variation of the mean PUP with vent offset in the 30 in. wetwell is shown in Figure 5-59. Again, in general, the mean PUP increases with vent offset as expected. However, due to the small magnitudes of the mean PUPs, and the measurement uncertainties of ± 1 psi, it is difficult to draw any further inferences regarding the data trends as could be done for the mean POPs discussed above.

The corresponding variation of the mean POP and PUP at the pool bottom elevation with vent offset is shown in Figures 5-60 and 5-61 respectively. In general, except for one or two data points, both the mean POP and PUP at this location also increase with increasing vent offset as expected. Vent offset has no effect on the chug frequency, as shown in Figure 5-62.

As mentioned earlier, vent offsets of 4 in. and 10 in. in the 18 in. and 30 in. wetwells respectively result in the same distance between the vent center and the 0° circumferential location as that for the centered vent in the 10 in. wetwell as shown in Figure 5-57. For these conditions with a constant 5 in. distance from the vent center to the wall, the mean POPs at the vent exit elevation 0° circumferential location and the pool bottom elevation are shown in Figures 5-63 and 5-64 respectively. Although the distances between the vent center and the transducer locations are the same, from the figures it is seen that the mean POPs for these three geometries differ. The highest mean POP was observed in the smallest wetwell and the lowest in the largest pool over the entire range of steam mass fluxes tested. The mean chug frequencies for these geometries are shown in Figure 5-65 which shows that the mean chug frequencies for the 10 in. wetwell geometry are slightly lower than those for the other geometries.

With the 6 in. offset vent in the 30 in. wetwell, the distance between the vent center and the 0° circumferential location is the same as that for the centered vent 18 in. wetwell geometry (see Figure 5-57). The mean POPs at the vent exit and pool bottom elevation for these two geometries as a function of the steam mass flux are shown in Figures 5-66 and 5-67 respectively. Again, the smaller wetwell—the 18 in. wetwell in this case—has the higher POPs. As shown in Figure 5-68, the mean chug frequencies for these geometries are nearly the same.

In summary, the vent offset tests have shown that POP decreases with both increased pool size (with constant vent-to-transducer spacing) and increased vent-to-transducer spacing (with constant pool size). Furthermore, the results of the tests of Section 5.5 are consistent with these observations; as pool size (and also vent-to-transducer distance) was increased with centered vents the wall mean POPs decreased faster ($1/D^2$) than with either size or spacing individually.

These data from the offset vent tests as well as the data from the previous section provide a means for understanding the mechanics of chug induced wave propagation in the pool. In addition, these data indicate that if the vents chug out-of-phase in a multivent geometry, the magnitude of the wall pressures at a given pool wall location will be lower than those in a corresponding single vent geometry due to the combined effects of pool size and vent location in the pool.

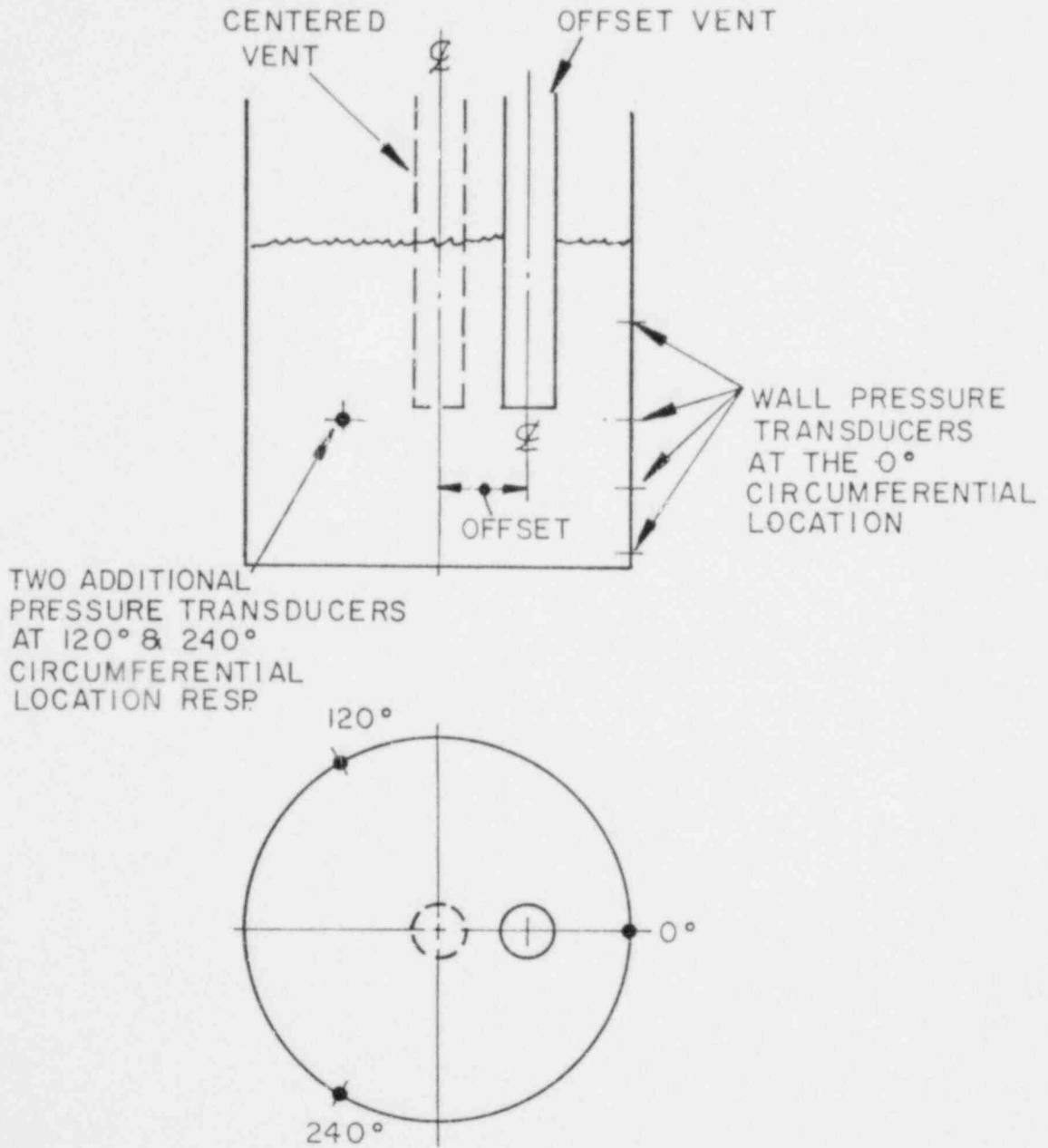


Figure 5-56. SCHEMATIC OF VENT OFFSET

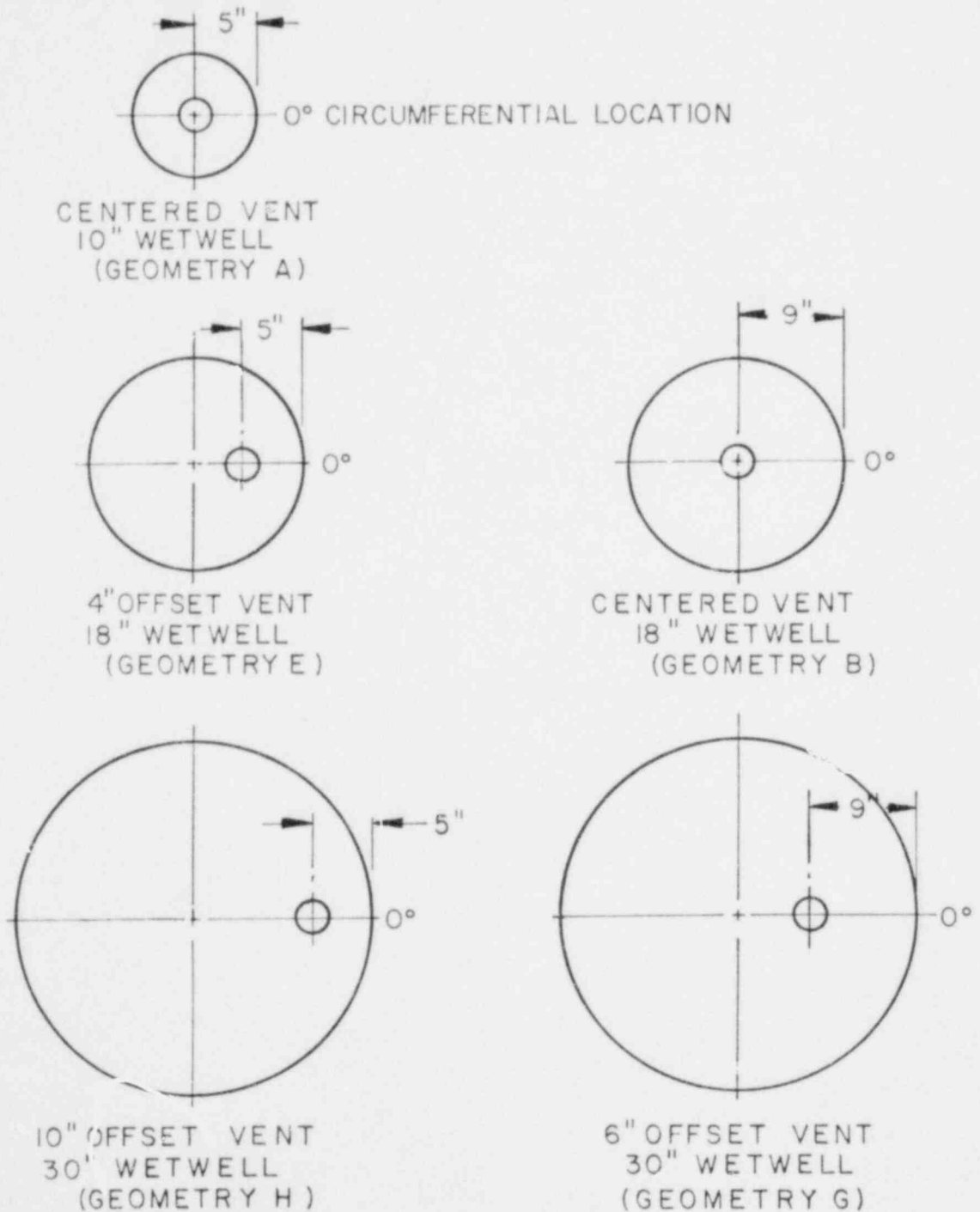


Figure 5-57. SCHEMATIC OF EQUIVALENT CENTERED AND OFFSET VENT GEOMETRIES

The following Figures are General Electric Company Proprietary and have been removed from this document in their entirety.

<u>Figure</u>	<u>Title</u>	<u>Page</u>
5-58	Variation of Mean POP at Vent Exit Elevation 0° Circumferential Location With Vent Offset in the 30 in. Wetwell	5-70
5-59	Variation of Mean PUP at Vent Exit Elevation 0° Circumferential Location With Vent Offset in the 30 in. Wetwell	5-71
5-60	Variation of Mean POP at Pool Bottom Elevation With Vent Offset in the 30 in. Wetwell	5-72
5-61	Variation of Mean PUP at Pool Bottom Elevation With Vent Offset in the 30 in. Wetwell	5-73
5-62	Variation of Mean Chug Frequency With Vent Offset in the 30 in. Wetwell	5-74
5-63	Variation of Mean POP at Vent Exit Elevation 0° Circumferential Location With Wetwell Size Keeping the Distance (5 in.) Between the Vent and Transducer Location Constant—1/10-Scale Single Vent Tests	5-75
5-64	Variation of Mean POP at the Pool Bottom Elevation With Wetwell Size Keeping the Distance (15 in.) Between the Vent and Transducer Location Constant—1/10-Scale Single Vent Tests	5-76
5-65	Variation of Mean Chug Frequency With Wetwell Size Keeping The Distance Between the Vent and Transducer Constant—1/10-Scale Single Vent Tests	5-77
5-66	Variation of Mean POP at Vent Exit Elevation 0° Circumferential Location With Wetwell Size Keeping the Distance (9 in.) Between the Vent and Transducer Constant—1/10-Scale Single Vent Tests	5-78
5-67	Variation of Mean POP at Pool Bottom Elevation With Wetwell Size Keeping the Distance (17 in.) Between the Vent and Transducer Constant—1/10-Scale Single Vent Tests	5-79
5-68	Variation of Mean Chug Frequency With Wetwell Size Keeping the Distance Between the Vent and Transducer Constant—1/10-Scale Single Vent Tests	5-80

6 TEST RESULTS AND DISCUSSION—MULTIVENT DATA AT 1/10 AND 1/6 SCALE

The multivent geometries tested in Phase 1 were the 1/10 scale 3 and 7 vent geometries and 1/6 scale 3 vent geometry. These three geometries provided the baseline multivent data which are compared with the single vent baseline data at 1/10 and 1/6 scale in the following sections.

In Section 6.1, the comparison between the single and multivent data is made in terms of the mean POP, PUP, chug frequency and the multivent multiplier. The multivent multiplier is defined as the ratio of the mean POPs in the multivent geometry and the corresponding single vent geometry at the same transducer location and test conditions. Vent phasing data were obtained for the 3 vent geometries and these data are discussed in Section 6.2. Two additional multivent geometries—1/10 and 1/6 scale 3 vent geometries with larger drywells—were tested to obtain the effect of drywell size on the multivent pool wall pressures. The data from these tests are discussed in Section 6.3.

The data presented in the following sections are mainly those obtained at the 45 psia wetwell airspace pressure, i.e., at the Mach scaled conditions. The data at the Froude scaled conditions exhibited anomalous trends. It appears that the most likely reason for this is the presence of uncontrolled amounts of air in the system due to the sub-ambient wetwell pressures at the Froude scaled conditions, as discussed in Section 5.

6.1 Multivent Pool Wall Pressures

General Characteristics

Sample traces for the pool bottom elevation pressure, vent static pressure, drywell pressure and the vent water level for the 1/10 scale single vent, 3 vent and 7 vent geometries at the same test conditions are shown in Figures 6-1, 6-2, and 6-3, respectively. The data shown were obtained at 4 lb/sec ft² steam mass flux, 130°F pool temperature, and the steam air content was zero. A comparison of the wall pressure trace at the pool bottom elevation shows that the magnitudes of the wall pressure oscillations due to chugging are lower for the multivent geometries. Also, the number of chugs observed in the 3 sec duration shown is larger for the multivent geometries at these test conditions.

The vent static pressure shown for the multivent geometries was for the vent at the 0° circumferential location. The vent static pressure oscillations are about the same for the single and multivent geometries—both in terms of the magnitudes and frequency. The similarity in the magnitudes of the vent static pressure indicates that the flow induced in the vent during a chug and hence the condensation rates were similar in all three geometries. The frequency of the vent static pressure oscillations is around 48 Hz and corresponds to the first harmonic of the vent (1/4 wave frequency). Note that the vent length for all three geometries was the same (9.47 ft).

The smallest drywell pressure oscillations occur in the 7 vent geometry which has the largest drywell volume since the drywell volume per vent was kept constant. The largest water excursions into the vent following a chug occur in the single vent geometry and decrease with increasing number of vents, as expected.

Sample data traces for the 1/6 scale single and 3 vent geometries at the same test conditions as those for the 1/10 scale data traces discussed above, are shown in Figures 6-4 and 6-5 respectively. All the observations made above for the 1/10 scale single and multivent data traces are also true for these 1/6 scale data traces.

Steam Mass Flux

The mean POPs for the 1/10 scale single, 3 and 7 vents geometries as a function of steam mass flux at a pool temperature of 130°F are shown in Figure 6-6. The variation in mean POP with steam mass flux is similar for all three geometries with the highest mean POPs occurring in the single vent geometry and decreasing with increasing number of vents. The same is true for the mean PUP shown in Figure 6-7. The mean pool chug frequency for these three geometries is shown in Figure 6-8. Again, all three geometries exhibit a similar trend with the mean chug frequency increasing almost linearly with steam mass flux. The chug frequency is somewhat higher for the multivent geometries than the single vent geometry.

The multivent multipliers at the pool bottom elevation for the three and seven vent geometries at various steam mass fluxes, 130°F pool temperature and 45 psia wetwell airspace pressure are shown in Figure 6-9. The uncertainty bands for the multivent multipliers are also shown on this figure. These uncertainty bands reflect the measurement uncertainties of ± 1 psi for the measurement system. Additional uncertainty in the mean values of the POP resulting from the statistical nature of chugging itself is not included in the uncertainty bands shown.

From Figure 6-9 it is seen that the multivent multiplier is less than one and decreases with increasing number of vents. Note that since the pool-to-vent area ratio was kept constant between the single and multivent geometries, the multivent multiplier would be very close to unity at any location in the pool if all the vents chugged in phase and with chug "source" strengths similar to those in a single vent geometry. The fact that the multivent multiplier is less than unity therefore implies that the vents chug out-of-phase and/or the chug "source" strength in a multivent geometry is less than that in a single vent geometry. As will be shown later, it appears that the most probable reason for the observed trend in the multivent multiplier is that the vents chug out-of-phase.

The multivent multipliers at the vent exit elevation for the 1/10 scale geometries are shown in Figure 6-10. The trends are similar to those observed for the pool bottom elevation location with some differences in the actual magnitudes of the multivent multipliers which are probably caused by the statistical nature of chugging.

The comparison between the single vent and multivent data at 1/6 scale are shown in Figures 6-11 through 6-14. Again, the data trends are similar to those observed previously at 1/10 scale with the mean POP and PUP for the multivent geometry lower than those for the single vent geometry. Also, the multivent multiplier (Figure 6-14) is less than one as was observed at 1/10 scale. Phase II will provide greater insight on the effect of scale since it includes 7 vent tests at 1/6 scale.

Pool Temperature

The effect of pool temperature on the multivent chugging at 1/10 scale is shown in Figures 6-15 through 6-17. It is seen that variations of the mean POP, PUP and chug frequency for the multivent geometries are similar to those for the corresponding single vent geometry. Again, over the range of pool temperatures tested, the mean POP and PUP are lower and the mean chug frequencies higher in the multivent geometries. These observations also hold for the 1/6 scale data shown in Figure 6-18 through 6-20.

The corresponding multivent multipliers for the 1/10 and 1/6 scale tests are shown in Figures 6-21 and 6-22 respectively. The multivent multipliers are less than one over the pool temperature range tested and as seen from the 1/10 scale data, the multivent multiplier decreases with increasing number of vents.

Air Content

The variations of the mean POP, PUP and chug frequency with steam air-content for the 1/10 and 1/6 scale single and multivent data are shown in Figures 6-23 through 6-25 and Figures 6-26 through 6-28, respectively. The wall pressures decrease with increasing steam air-content similar to those for the single vent. Air-content has no significant effect on the mean chug frequency. The corresponding multivent multipliers at 1/10 and 1/6 scale are shown in Figures 6-29 and 6-30, respectively. Again, the multivent multiplier is less than one and decreases with increasing number of vents.

Summary

In summary, the overall characteristics of wall pressures due to multivent chugging are similar to those for single vent chugging. The variation of the mean POP, PUP and chug frequency with the important thermodynamic parameters—steam mass flux, pool temperatures, and steam air-content—are also similar for the single and multivent geometries. The main difference between single vent and multivent wall pressures is that the magnitude of the mean POP and PUP is lower for the multivent geometries, i.e., the multivent multiplier is less than one. Finally, the multivent multiplier decreases with increasing number of vents.

The following Figures are General Electric Proprietary and have been removed from this document in their entirety.

<u>Figure</u>	<u>Title</u>	<u>Page</u>
6-1	Data Traces—1/10-Scale Single Vent Test	6-4
6-2	Data Traces—1/10-Scale 3 Vent Test	6-5
6-3	Data Traces—1/10-Scale 7 Vent Test	6-6
6-4	Data Traces—1/6-Scale Single Vent Test	6-7
6-5	Data Traces—1/6-Scale 3 Vent Test	6-8
6-6	Variation of Mean POP at Pool Bottom Elevation With Number of Vents—1/10-Scale Single and Multivent Tests	6-9
6-7	Variation of Mean PUP at Pool Bottom Elevation With Number of Vents—1/10-Scale Single and Multivent Tests	6-10
6-8	Variation of Mean Chug Frequency With Number of Vents—1/10-Scale Single and Multivent Tests	6-11
6-9	Multivent Multiplier (Mean POP) at Pool Bottom Elevation—1/10-Scale Single and Multivent Tests	6-12
6-10	Multivent Multiplier (Mean POP) at Vent Exit Elevation—1/10 Scale Single and Multivent Tests	6-13
6-11	Variation of Mean POP at Pool Bottom Elevation With Number of Vents—1/6-Scale Single and Multivent Tests	6-14
6-12	Variation of Mean PUP at Pool Bottom Elevation With Number of Vents—1/6-Scale Single and Multivent Tests	6-15
6-13	Variation of Mean Chug Frequency With Number of Vents—1/6-Scale Single and Multivent Tests	6-16
6-14	Multivent Multiplier (Mean POP) at Pool Bottom Elevation—1/6-Scale Single and Multivent Tests	6-17
6-15	Variation of Mean POP at Pool Bottom Elevation With Number of Vents—1/10 Scale Single and Multivent Tests	6-18
6-16	Variation of Mean PUP at Pool Bottom Elevation With Number of Vents—1/10-Scale Single and Multivent Tests	6-19
6-17	Variation of Mean Chug Frequency With Number of Vents—1/10-Scale Single and Multivent Tests	6-20
6-18	Variation of Mean POP at Pool Bottom Elevation With Number of Vents—1/6 Scale Single and Multivent Tests	6-21
6-19	Variation of Mean PUP at Pool Bottom Elevation With Number of Vents—1/6-Scale Single and Multivent Tests	6-22
6-20	Variation of Mean Chug Frequency With Number of Vents—1/6-Scale Single and Multivent Tests	6-23
6-21	Multivent Multiplier (Mean POP) at Pool Bottom Elevation—1/10-Scale Single and Multivent Tests	6-24
6-22	Multivent Multiplier (Mean POP) at Pool Bottom Elevation—1/6-Scale Single and Multivent Tests	6-25
6-23	Variation of Mean POP at Pool Bottom Elevation With Number of Vents—1/10-Scale Single and Multivent Tests	6-26
6-24	Variation of Mean PUP at Pool Bottom Elevation With Number of Vents—1/10-Scale Single and Multivent Tests	6-27

<u>Figure</u>	<u>Title</u>	<u>Page</u>
6-25	Variation of Mean Chug Frequency With Number of Vents—1/10-Scale Single and Multivent Tests	6-28
6-26	Variation of Mean POP at Pool Bottom Elevation With Number of Vents—1/6-Scale Single and Multivent Tests	6-29
6-27	Variation of Mean PUP at Pool Bottom Elevation With Number of Vents—1/6-Scale Single and Multivent Tests	6-30
6-28	Variation of Mean Chug Frequency With Number of Vents—1/6-Scale Single and Multivent Tests	6-31
6-29	Multivent Multiplier (Mean POP) at Pool Bottom Elevation—1/10 Scale Single and Multivent Tests	6-32
6-30	Multivent Multiplier (Mean POP) at Pool Bottom Elevation—1/6-Scale Single and Multivent Tests	6-33

6.2 Vent Phasing

A chug is said to have occurred when the oscillations in the pool wall pressure exceed a given threshold. In a multivent geometry such a chug (called a "pool" chug) can be due to chugs at one, some, or all of the individual vents. An algorithm was developed (described in Section 3.2) which was used to determine the number and timing of individual vents that chugged during a given "pool" chug. This algorithm used the vent static pressure and water level in individual vents to obtain these phasing data. Since only three vents in a multivent geometry were instrumented, phasing data were obtained for the three vent geometries only. In a given three vent test, the phasing algorithm was used to obtain the percentages of pool chugs due to chugs at one, two or all three vents. For pool chugs consisting of two or three individual vents chugging, the average time delay between the first and last vent to chug was also computed.

The percentages of pool chugs comprising of one, two and three vents for the 1/10 scale three vent geometry are shown in Figures 6-31, 6-32, and 6-33 respectively. It is seen that at the lower steam mass fluxes, a significant number of pool chugs are due to one or two individual vents chugging. At higher steam mass fluxes, almost all the pool chugs are due to all three vents chugging. The same is true for the 1/6 scale three vent geometry as shown in Figures 6-34, 6-35 and 6-36.

The delay time for the pool chugs due to two individual vents chugging for the 1/10 and 1/6 scale three vent geometries are shown in Figures 6-37 and 6-38 respectively. In general, this time delay is about 0.02 seconds. Similarly, the delay times for pool chugs due to all three vents chugging for the 1/10 and 1/6 scale three vent geometries are shown in Figures 6-39 and 6-40 respectively. The average delay time between the chugs at the first and the last vent when three vents chugged tended to be slightly longer on average than for two vents.

The important point to be noted here is that for the three vent geometries tested, not all vents chug during a given pool chug, especially at low steam mass fluxes. Further, the chugs at individual vents during a pool chug are out-of-phase. These observations provide at least a partial reason for the reduction in pool wall pressure magnitudes observed in the multivent geometries (i.e., for multivent multipliers being less than one). Since the vents chug out-of-phase in a multivent geometry, in effect, the vents chug individually in the larger multivent pool. As discussed earlier in Section 5.5, the effect of larger pool size is to reduce the magnitudes of the wall pressures. Therefore, the reduced multivent pool wall pressures are due to the effectively larger pool in which the individual vents chug in a multivent geometry. Note that the multivent wall pressures would be the same as those for the single vent geometry if all vents in the multivent geometry chugged in-phase.

A comparison is shown in Figure 6-41 between the mean POP for the 1/10 scale three vent geometry and the geometry with the 1/10 scale single vent in the 18 in. diameter pool (the same pool as used in the 1/10 scale three vent geometry). It is seen that the mean POPs for the two geometries show very good agreement. This lends considerable credence to the hypothesis that the observed reduction in pool wall pressures in a multivent geometry is due to the pool size effect with the vents chugging out-of-phase.

The following Figures are General Electric Company Proprietary and have been removed from this document in their entirety.

<u>Figure</u>	<u>Title</u>	<u>Page</u>
6-31	Percent of One Vent Pool Chugs—1/10-Scale 3 Vent Tests	6-35
6-32	Percent of Two Vent Pool Chugs—1/10-Scale 3 Vent Tests	6-36
6-33	Percent of Three Vent Pool Chugs—1/10-Scale 3 Vent Tests	6-37
6-34	Percent of One Vent Pool Chugs—1/6-Scale 3 Vent Tests	6-38
6-35	Percent of Two Vent Pool Chugs—1/6-Scale 3 Vent Tests	6-39
6-36	Percent of Three Vent Pool Chugs—1/6-Scale 3 Vent Tests	6-40
6-37	Average Time Delay Between the First and Last Vent To Chug in Two Vent Pool Chugs—1/10-Scale 3 Vent Tests	6-41
6-38	Average Time Delay Between the First and Last Vent to Chug in Two Vent Pool Chugs—1/6-Scale 3 Vent Tests	6-42
6-39	Average Time Delay Between the First and Last Vent to Chug in Three Vent Pool Chugs—1/10-Scale 3 Vent Tests	6-43
6-40	Average Time Delay Between the First and Last Vent to Chug in Three Vent Pool Chugs—1/6-Scale 3 Vent Tests	6-44
6-41	Comparison of Mean POPs at Pool Bottom Elevation for the Centered Single Vent and Three Vents in the Same Size Wetwell—1/10-Scale Single and Multivent Tests	6-45

6.3 Effect of Drywell Volume

The 1/10 and 1/6 scale three vent geometries were tested with an oversized drywell in addition to the scaled drywell, to see if the drywell volume had any effect on the characteristics of multivent chugging. Figures 6-42 through 6-44 show the comparison of mean POP, PUP and chug frequency for the 1/10 scale three vent geometry with the scaled (7.3 ft³) and larger drywell (32.0 ft³). From these figures it is seen that increasing the drywell volume has no significant effect on either the mean POP or PUP for steam mass fluxes up to 4 lb/sec ft². At the two higher steam mass fluxes, the mean POP and PUP are slightly lower for the larger drywell geometry. The mean chug frequency is identical for both geometries indicating that increasing the drywell size has no effect on the mean chug frequency. These observations also hold at 1/6 scale as shown in Figures 6-45 through 6-47.

In closing, it is noted that the effects of larger drywell size on multivent chugging discussed above are identical to those observed for the single vent chugging (see Section 5.4).

The following Figures are General Electric Company Proprietary and have been removed from this document in their entirety.

<u>Figure</u>	<u>Title</u>	<u>Page</u>
6-42	Effect of Drywell Volume on Mean POP at Pool Bottom Elevation- 1/10-Scale 3 Vent Tests	6-47
6-43	Effect of Drywell Volume on Mean PUP at Pool Bottom Elevation- 1/10-Scale 3 Vent Tests	6-48
6-44	Effect of Drywell Volume on Mean Chug Frequency—1/10-Scale 3 Vent Tests	6-49
6-45	Effect of Drywell Volume on Mean POP at Pool Bottom Elevation- 1/6-Scale 3 Vent Tests	6-50
6-46	Effect of Drywell Volume on Mean PUP at Pool Bottom Elevation- 1/6-Scale 3 Vent Tests	6-51
6-47	Effect of Drywell Volume of Mean Chug Frequency—1/6-Scale 3 Vent Tests	6-52

7 CONCLUSIONS

A substantial single vent and multivent data base has been obtained in Phase 1 of the Scaled Multivent Test Program. The data trends observed in the data for tests at ambient and 45 psia wetwell airspace pressure are remarkably clear and consistent between the 1/10 and 1/6 scale geometries.

The major conclusions drawn from the Phase 1 single vent data presented in Section 5 are:

- 1) The behavior of the mean POP, PUP and chug frequency with steam mass flux, pool temperature and air content was similar at both 1/10 and 1/6 scales and consistent with that observed in previous single vent tests [2]. The mean POP was found to increase with steam mass flux. The mean chug frequency was found to be directly proportional to the steam mass flux. For a given steam mass flux, mean POP reaches a maximum at some value of the pool temperature; and the pool temperature had no significant effect on the mean chug frequency in the range of pool temperatures tested. The mean POP decreases with increasing steam air-content; at a given steam mass flux, steam air-content has no significant effect on the mean chug frequency.
- 2) Increasing the drywell volume has no effect on the mean POP at steam mass fluxes < 4 lb/sec ft². A small decrease in mean POP is observed with increased drywell size at steam mass fluxes of 8 and 16 lb/sec ft². Increasing the drywell volume has no effect on the mean chug frequency.
- 3) The mean POP is inversely proportional to the pool area. This implies that mean POP in a multivent geometry will be considerably lower than that in a corresponding single vent geometry if the vents chug out-of-phase in the multivent geometry. The mean chug frequency increases slightly with increasing pool size.
- 4) The wall pressure at a given pool location increases as the vent is moved closer to it. A detailed comparison of these data with predictions from acoustic models of the pool should provide a good check on the validity of the assumption that wave propagation in the pool can be modeled using the acoustic equation.

The major conclusions drawn from the Phase 1 multivent data presented in Section 6 are:

- 1) Overall characteristics of multivent chugging are similar to those of single vent chugging—the trends of the mean POP, PUP and chug frequency with steam mass flux, pool temperature and steam air-content are similar for single vent and multivent chugging.
- 2) The pool wall pressures in the multivent geometries are lower than those in the corresponding single vent geometry. That is, the multivent multiplier is less than one. Further, the multivent multiplier decreases with increasing number of vents.
- 3) In the 3-vent geometries for which vent phasing data were obtained, the vents chug out-of-phase. The average time delay between the first and last vent to chug in a "pool chug" is about 0.02 sec. Since the vents chug out-of-phase, the most probable reason for the reduced wall pressures in the multivent geometry is the effectively larger pool size that individual vents see.

- 4) The effect of increasing drywell size in a multivent geometry is similar to that in the single vent geometry. Increase in drywell volume reduces the mean POP slightly at steam mass fluxes of 8 and 16 lb/sec ft²; no significant effect on mean POP at lower steam mass fluxes was observed. The mean chug frequency is unaffected by an increase in the drywell volume.

In closing, the Phase 1 single vent and multivent data support the assertion that single cell pool wall pressures are greater than those expected in a multivent geometry. Further, the Phase 1 data base provides a means for verifying some of the modeling assumptions used by the improved load definition methodology.

8 REFERENCES

- 1) Grafton, W. A., McIntyre, T. R. and Ross, M. A.; MARK II PRESSURE SUPPRESSION TEST PROGRAM, PHASE II AND III TESTS; NEDE-13468-P, General Electric Company, October 1976 (Proprietary).
- 2) Patel, B. R., Block, J. A. and Stacy, W. D.; PARAMETRIC STUDY OF CHUGGING BEHAVIOR; Creare Technical Report TN-267, September 1977.
- 3) Bilanin, W. J., et. al.; MARK II LEAD PLANT TOPICAL REPORT - POOL BOUNDARY AND MAIN VENT CHUGGING LOADS JUSTIFICATION; NEDO-23617, General Electric Company, July 1977.
- 4) Clabaugh, W. J.; SCALED MULTIVENT TEST PROGRAM PLAN (PHASE 1 TESTS); NEDO-23697A Revision 1, General Electric Company, January 1979.
- 5) Clabaugh, W. J.; SCALED MULTIVENT TEST PROGRAM PLAN (PHASE 2 TESTS); NEDO-23697A Revision 1, Supplement 1, General Electric Company, September 1979.
- 6) Fluid Meters - Their Theory and Application; 6th Edition, ASME 1971.
- 7) Dolan, F. X. and Patel, B. R.; PHASE 1 TEST PLAN AND PROCEDURE; Revision 1, August 1978.
- 8) Chan, C. K., et. al.; SUPPRESSION POOL DYNAMICS; NUREG-0264-3, June 1977.
- 9) Anderson, W. G., Huber, P. W. and Sonin, A. A.; SMALL SCALE MODELING OF HYDRODYNAMIC FORCES IN PRESSURE SUPPRESSION SYSTEMS; NUREG/CR-0003, March 1978.
- 10) Patel, B. R., Dolan, F. X. and Block, J. A.; CONMAP TESTS EXPERIMENTAL DATA REPORT; Creare Technical Note TN-297, June 1979.

NEDO-2478 1-1